

*Round and round and round she goes,  
And where she stops, nobody knows.*

Origin unknown, used in *The Original Amateur Hour*, radio and TV program, 1934–1970.

## CHAPTER 15

# Zonally-Averaged Mid-Latitude Atmospheric Circulation

**T**HE FOCUS OF THIS CHAPTER is the zonally-averaged structure and circulation of the extratropical troposphere. Because of the presence of strong zonal asymmetries — in particular baroclinic eddies or, more simply, the weather — this circulation differs markedly from the zonally *symmetric* circulation that would exist if eddies did not develop at all. The angular-momentum-conserving model of the Hadley Cell discussed in Chapter 14 is an example of a zonally-symmetric circulation, but this may be quite different from the zonally-*averaged* circulation in a turbulent atmosphere. Let us explain more.

When studying some aspects of the large-scale ocean circulation, or the low-latitude atmospheric circulation, we can make a great deal of progress by treating the large-scale flow as if it were absolutely steady with the eddies having only a perturbative effect. However, this approach fails badly for the mid-latitude atmosphere: the large-scale mid-latitude circulation is intrinsically unsteady on the large-scale to the extent that the associated eddies essentially *are* the circulation. The eddies are also unpredictable and chaotic; that is to say, *the large-scale mid-latitude circulation of the atmosphere is a turbulent flow*. This turbulence involves large-scale, geostrophically and hydrostatically balanced flow — that is, it is geostrophic turbulence — and so has different properties than the smaller-scale, more nearly three-dimensional turbulence that may occur in boundary layers and the like. Further, this large-scale turbulence (sometimes called ‘macro-turbulence’) is neither fully-developed nor isotropic — it interacts with the Rossby waves that arise from the planetary rotation and might be regarded as a form of weak turbulence. Why is the large-scale flow turbulent? Why is it zonally asymmetric at all? There are two potential sources for zonal asymmetries:

- (i) The zonal asymmetries that exist in the underlying boundary conditions and forcing: mountains, land–sea contrasts, the diurnal cycle, and so on.
- (ii) Hydrodynamic instability: even if the surface and the forcing were exactly zonally symmetric, the corresponding zonally symmetric solutions of the equations of motion would have a large shear in the zonal wind and this might be baroclinically unstable to zonally asymmetric perturbations.

If the flow were not unstable, then we might expect that the zonal asymmetries of item (i) would give rise to corresponding, steady, zonal asymmetries in the resulting circulation, and this process

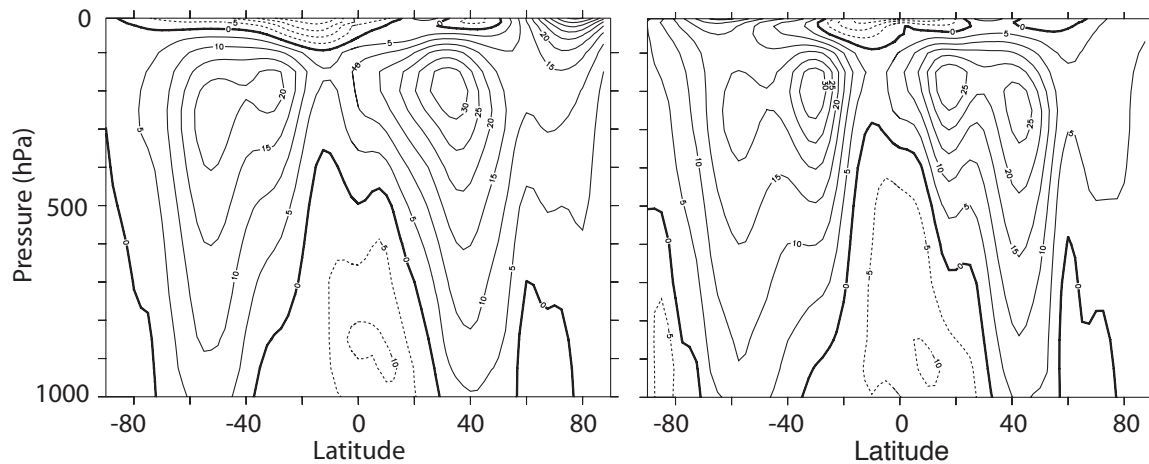


**Fig. 15.1** The time averaged zonal wind at 150° W (in the mid-Pacific) in December–January–February (DJF, left), March–April–May (MAM, right). The contour interval is  $5 \text{ m s}^{-1}$ . Note the double jet in each hemisphere, one in the subtropics and one in mid-latitudes. The subtropical jets are associated with a strong meridional temperature gradient, whereas the mid-latitude, eddy-driven, jets have a stronger barotropic component and are associated with westerly winds at the surface.

is discussed in the next chapter. However, the flow is unstable, primarily via baroclinic instability (as discussed in Chapter 9), and this leads to eddy growth and ultimately to geostrophic turbulence; this is, essentially, what gives rise to *weather*. The large-scale circulation is not, however, so turbulent that such things as Rossby waves cease to have meaning. Indeed, the most important nonlinear interactions are those involving Rossby waves and the zonally-averaged flow, and ideas of wave–mean–flow interaction go a long way in explaining the generation of the zonally-averaged flow. In particular, it is this interaction that produces the momentum convergence that gives rise to surface wind pattern.

In this chapter we focus on the effects of item (ii), and try to understand the mid-latitude circulation of an atmosphere with zonally symmetric forcing and boundary conditions. We assume that the zonal asymmetries due to the boundary conditions do not *qualitatively* affect our arguments, and that the circulation of the atmosphere with a perfectly smooth surface would resemble that of the real circulation. We will present our arguments semi-independently of earlier chapters, and in particular we will develop some of the results of wave–mean flow interaction *ab initio*, so that a reader with just a little experience can start here and refer back to these chapters as needed. We begin with a discussion of the mechanisms that maintain the surface westerlies.<sup>1</sup>

## 15.1 SURFACE WESTERLIES AND THE MAINTENANCE OF A BAROTROPIC JET

### 15.1.1 Observations and Motivation

The atmosphere above the surface has a generally eastward flow, with a broad maximum about 10 km above the surface at around 40° in either hemisphere. But if we look a little more at the zonally average wind in Fig. 14.2(a) we see hints of there being two jets — one (the subtropical jet) at around 30°, and another somewhat poleward of this, especially apparent in the Southern Hemisphere. Such a jet is particularly noticeable in certain regions of the globe, when a zonal average is not taken, as in Fig. 15.1. The subtropical jet is associated with a strong meridional temperature gradient at the edge of the Hadley Cell, and is quite baroclinic. On the other hand, the mid-latitude jet (sometimes called the subpolar jet) is more barotropic (it has little vertical structure, with less shear than the subtropical jet) and lies above an eastward surface flow. This

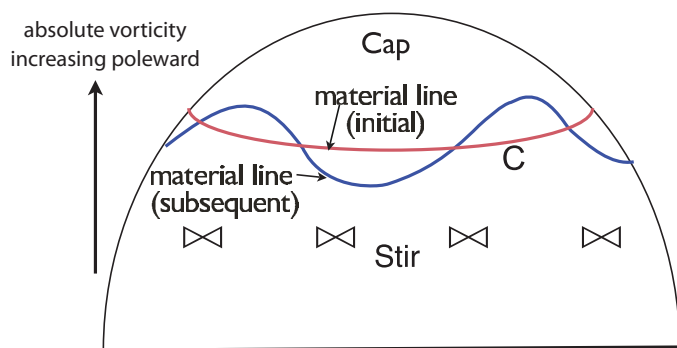


**Fig. 15.2** Sketch of the effects of a mid-latitude disturbance on the circulation around the latitude line C.

If initially the absolute vorticity increases monotonically poleward, then the disturbance will bring fluid with lower absolute vorticity into the cap region. Then, using Stokes theorem, the velocity around the latitude line C will become more westward.

flow feels the effect of friction and so there must be a momentum *convergence* into this region, as is seen in Fig. 14.12. We will find that this momentum convergence occurs largely in transient eddies, and the jet is known as the *eddy-driven jet*. Although the eddies are a product of baroclinic instability, the essential mechanism of jet production is present in barotropic dynamics, so we first consider how an eastward jet can be maintained in a turbulent two-dimensional flow on the surface of a rotating sphere.

In barotropic turbulence, alternating east–west jets can be maintained if  $\beta$  is non-zero, as described in Section 12.1. However, that case was homogeneous, with no preferred latitude for a particular direction of jet, whereas in the atmosphere there appears to be but one mid-latitude jet, and although it meanders it certainly has a preferred average location. In the subsections that follow we give four explications as to how the jet is maintained; the first has a different flavour from the others, but they are all really just different perspectives on the same mechanism; they are all the same explanation.<sup>2</sup>

### 15.1.2 The Mechanism of Jet Production

#### 1. The vorticity budget

Suppose that the absolute vorticity normal to the surface (i.e.,  $\zeta + 2\Omega \sin \vartheta$ ) increases monotonically poleward. (A sufficient condition for this is that the fluid is at rest.) By Stokes' theorem, the circulation around a line of latitude circumscribing the polar cap,  $I$ , is equal to the integral of the absolute vorticity over the cap. That is,

$$I_i = \int_{\text{cap}} \omega_{ia} \cdot d\mathbf{A} = \oint_C u_{ia} dl = \oint_C (u_i + \Omega a \cos \vartheta) dl, \quad (15.1)$$

where  $\omega_{ia}$  and  $u_{ia}$  are the initial absolute vorticity and velocity, respectively,  $u_i$  is the initial zonal velocity in the Earth's frame of reference, and the line integrals are around the line of latitude. For simplicity let us take  $u_i = 0$  and suppose there is a disturbance equatorward of the polar cap, and that this results in a distortion of the material line around the latitude circle C (Fig. 15.2). Since we are supposing the source of the disturbance to be distant from the latitude of interest, then if we neglect viscosity the circulation along the material line is conserved, by Kelvin's circulation theorem. Thus, vorticity with a lower value is brought into the region of the polar cap — that is, the region poleward of the latitude line C. Using Stokes' theorem again the circulation around the latitude circle C must therefore fall; that is, denoting values after the disturbance with a subscript  $f$ ,

$$I_f = \int_{\text{cap}} \omega_{fa} \cdot d\mathbf{A} < I_i \quad (15.2)$$

so that

$$\oint_C (u_f + \Omega a \cos \vartheta) dl < \oint_C (u_i + \Omega a \cos \vartheta) dl, \quad (15.3)$$

and

$$\bar{u}_f < \bar{u}_i, \quad (15.4)$$

with the overbar indicating a zonal average. Thus, there is a tendency to produce *westward* flow poleward of the disturbance. By a similar argument westward flow is also produced equatorward of the disturbance — to see this one might apply Kelvin's theorem over all of the globe south of the source of the disturbance (taking care to take the dot-product correctly between the direction of the vorticity vector and the direction normal to the surface). Finally, note that the overall situation is the same in the Southern Hemisphere. Thus, on the surface of a rotating sphere, external stirring will produce westward flow *away* from the region of the stirring.

Now suppose, furthermore, that the disturbance imparts no net angular momentum to the fluid. Then the integral of  $ua \cos \vartheta$  over the entire hemisphere must be constant. But the fluid is accelerating westward away from the disturbance. Therefore, the fluid in the region of the disturbance must accelerate *eastward*; that is, angular momentum must converge into the stirred region, producing an eastward flow. This simple mechanism is the essence of the production of eastward eddy-driven jets in the atmosphere, and of the eastward surface winds in mid-latitudes. The stirring that here we have externally imposed comes, in reality, from baroclinic instability.

If the stirring subsides then the flow may reversibly go back to its initial condition, with a concomitant reversal of the momentum convergence that caused the zonal flow. Thus, we must have some form of dissipation and irreversibility in order to produce permanent changes, and in particular we need to irreversibly mix vorticity. (This result is closely related to the non-acceleration results of Chapter 10.) If the fluid is continuously mixed, then we also need a source that restores the absolute vorticity gradient, otherwise we will completely homogenize the vorticity over the hemisphere.

## II. Rossby waves and momentum flux

We saw above that a mean gradient of vorticity is an essential ingredient in the mechanism whereby a mean flow is generated by stirring. Given such, we expect Rossby waves to be excited, and we now show how Rossby waves are intimately related to the momentum flux maintaining the mean flow.

If a stirring is present in mid-latitudes then we expect that Rossby waves will be generated there, propagate away and break and dissipate. To the extent that the waves are quasi-linear and do not interact, then just away from the source region each wave has the form

$$\psi = \text{Re } C e^{i(kx + ly - \omega t)} = \text{Re } C e^{i(kx + ly - kct)}, \quad (15.5)$$

where  $C$  is a constant, with dispersion relation

$$\omega = ck = \bar{u}k - \frac{\beta k}{k^2 + l^2} \equiv \omega_R, \quad (15.6)$$

provided that there is no meridional shear in the zonal flow. The meridional component of the group velocity is given by

$$c_g^y = \frac{\partial \omega}{\partial l} = \frac{2\beta kl}{(k^2 + l^2)^2}. \quad (15.7)$$

Now, the direction of the group velocity must be *away* from the source region; this is a radiation condition (discussed more in the next subsection), demanded by the requirement that Rossby waves transport energy *away* from the disturbance. Thus, northward of the source  $kl$  is positive

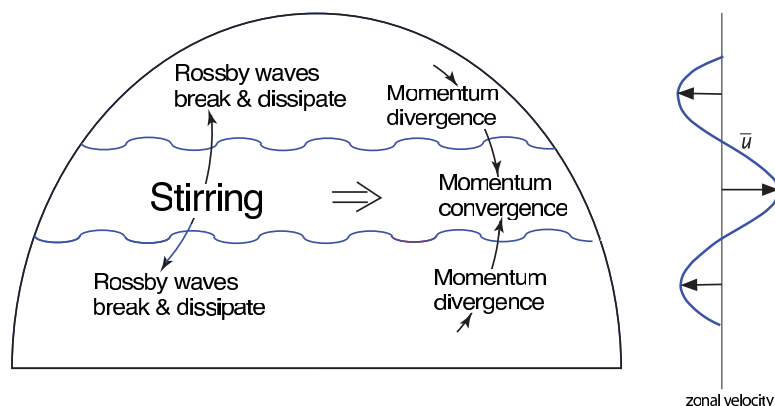


**Fig. 15.3** Generation of zonal flow on a rotating sphere.

Stirring in mid-latitudes (by baroclinic eddies) generates Rossby waves that propagate away. Momentum converges in the region of stirring, producing eastward flow there and weaker westward flow on its flanks.

and southward of the source  $kl$  is negative. That the product  $kl$  can be positive or negative arises because for each  $k$  there are two possible values of  $l$  that satisfy the dispersion relation (15.6), namely

$$l = \pm \left( \frac{\beta}{\bar{u} - c} - k^2 \right)^{1/2}, \quad (15.8)$$

assuming that the quantity in parentheses is positive.

The velocity variations associated with the Rossby waves are

$$u' = -\text{Re } C i l e^{i(kx+ly-\omega t)}, \quad v' = \text{Re } C i k e^{i(kx+ly-\omega t)}, \quad (15.9a,b)$$

and the associated momentum flux is

$$\overline{u'v'} = -\frac{1}{2} C^2 k l. \quad (15.10)$$

Thus, given that the sign of  $kl$  is determined by the group velocity, northward of the source the momentum flux associated with the Rossby waves is southward (i.e.,  $\overline{u'v'}$  is negative), and southward of the source the momentum flux is northward (i.e.,  $\overline{u'v'}$  is positive). That is, the momentum flux associated with the Rossby waves is *toward* the source region. Momentum converges in the region of the stirring, producing net eastward flow there and westward flow to either side (Fig. 15.3).

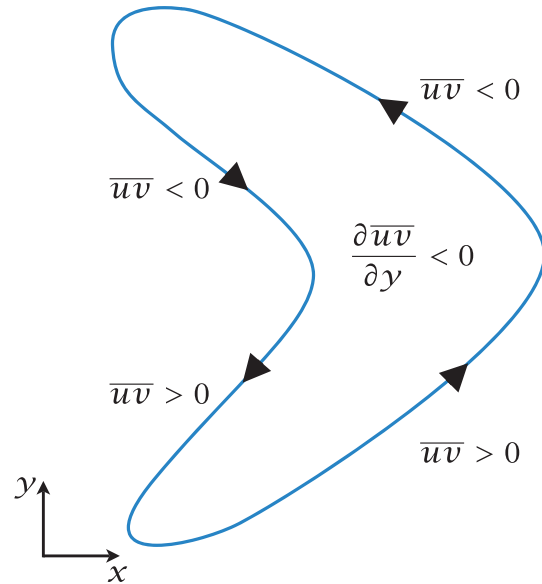
Another way of describing the same effect is to note that if  $kl$  is positive then lines of constant phase ( $kx + ly = \text{constant}$ ) are tilted north-west/south-east, and the momentum flux associated with such a disturbance is negative ( $\overline{u'v'} < 0$ ). Similarly, if  $kl$  is negative then the constant-phase lines are tilted north-east/south-west and the associated momentum flux is positive ( $\overline{u'v'} > 0$ ). The net result is a convergence of momentum flux into the source region. In physical space this is reflected by having eddies that are 'bow-shaped', as in Fig. 15.4.

#### ♦ The radiation condition and Rayleigh friction

Why is the group velocity directed away from the source region? It is because the energy flux travels at the group velocity, and the energy flux must be directed away from the source region; the reader comfortable with that statement may stop here. (See Section 6.7 for more on group velocity.) Another way to determine the direction of the group velocity is to employ a common trick in problems of wave propagation, that of adding a small amount of friction to the inviscid problem.<sup>3</sup> The solution of the ensuing problem in the limit of small friction will often make clear which solution is physically meaningful in the inviscid problem, and therefore which solution nature chooses. Consider the linear barotropic vorticity equation with linear friction,

$$\frac{\partial \zeta}{\partial t} + \beta \frac{\partial \psi}{\partial x} = -r \zeta, \quad (15.11)$$

**Fig. 15.4** The momentum transport in physical space, caused by the propagation of Rossby waves away from a source in mid-latitudes. The ensuing bow-shaped eddies are responsible for a convergence of momentum, as indicated. If the arrows were reversed the momentum transport would still have the same sign.



where  $r$  is a small friction coefficient. The dispersion relation is

$$\omega = -\frac{\beta k}{K^2} - ir = \omega_R(k, l) - ir, \quad (15.12)$$

where  $\omega_R$  is defined by (15.6), with  $\bar{u} = 0$ , and so the wave decays with time. Now suppose a wave is generated in some region, and that it propagates meridionally away, decaying as it moves away. Then, instead of an imaginary frequency, we may suppose that the frequency is real and the  $y$ -wavenumber is imaginary. Specifically, we take  $l = l_0 + l'$ , where  $l_0 = \pm[\beta/(\bar{u} - c) - k^2]^{1/2}$  for some zonal wavenumber  $k$ , as in (15.8), and  $\omega = \omega_R(k, l_0)$ . For small friction, we obtain  $l'$  by Taylor-expanding the dispersion relation around its inviscid value,  $\omega_R(k, l_0)$ , giving

$$\omega + ir = \omega_R(k, l) \approx \omega_R(k, l_0) + \left. \frac{\partial \omega_R(k, l)}{\partial l} \right|_{l=l_0} l', \quad (15.13)$$

and therefore

$$l' = \frac{ir}{c_g^y}, \quad (15.14)$$

where  $c_g^y = \partial_l \omega_R(k, l)|_{l=l_0}$  is the  $y$ -component of the group velocity. The wavenumber is imaginary, so that the wave either grows or decays in the  $y$ -direction, and the wave solution obeys

$$\psi \approx \text{Re } C \exp[i(kx - \omega_R t)] \exp(il_0 y - r y/c_g^y). \quad (15.15)$$

We now demand that the solution decay away from the source, because any other choice is manifestly unphysical, even as we let  $r$  be as small as we please. Thus, with the source at  $y = 0$ ,  $c_g^y$  must be positive for positive  $y$  and negative for negative  $y$ . In other words, the group velocity must be directed *away* from the source region, and so momentum flux converges on the source region.

### III. The pseudomomentum budget

The kinematic relation between vorticity flux and momentum flux for non-divergent two-dimensional flow is

$$v\zeta = \frac{1}{2} \frac{\partial}{\partial x} (v^2 - u^2) - \frac{\partial}{\partial y} (uv). \quad (15.16)$$

After zonal averaging this gives

$$\overline{v'\zeta'} = -\frac{\partial \overline{u'v'}}{\partial y}, \quad (15.17)$$

noting that  $\bar{v} = 0$  for two-dimensional incompressible (or geostrophic) flow. In spherical coordinates this expression becomes

$$\overline{v'\zeta'} \cos \vartheta = -\frac{1}{a \cos \vartheta} \frac{\partial}{\partial \vartheta} (\cos^2 \vartheta \overline{u'v'}). \quad (15.18)$$

If either (15.17), or (15.18) are integrated with respect to  $y$  between two quiescent latitudes then their right-hand sides vanish. That is the zonally-averaged meridional vorticity flux vanishes when integrated over latitude.

Now, the barotropic zonal momentum equation is (for horizontally non-divergent flow)

$$\frac{\partial u}{\partial t} + \frac{\partial u^2}{\partial x} + \frac{\partial uv}{\partial y} - fv = -\frac{\partial \phi}{\partial x} + F_u - D_u, \quad (15.19)$$

where  $F_u$  and  $D_u$  represent the effects of any forcing and dissipation. Zonal averaging, with  $\bar{v} = 0$ , gives

$$\frac{\partial \bar{u}}{\partial t} = -\frac{\partial \bar{u}\bar{v}}{\partial y} + \bar{F}_u - \bar{D}_u, \quad \text{or} \quad \frac{\partial \bar{u}}{\partial t} = \overline{v'\zeta'} + \bar{F}_u - \bar{D}_u. \quad (15.20)$$

using (15.17). Thus, the zonally-averaged wind is maintained by the zonally-averaged vorticity flux. On average there is little if any direct forcing of horizontal momentum and we may set  $\bar{F}_u = 0$ , and if the dissipation is parameterized by a linear drag (15.20) becomes

$$\frac{\partial \bar{u}}{\partial t} = \overline{v'\zeta'} - r\bar{u}, \quad (15.21)$$

where the constant  $r$  is an inverse frictional time scale.

Now consider the maintenance of this vorticity flux. The barotropic vorticity equation is

$$\frac{\partial \zeta}{\partial t} + \mathbf{u} \cdot \nabla \zeta + v\beta = F_\zeta - D_\zeta, \quad (15.22)$$

where  $F_\zeta$  and  $D_\zeta$  are forcing and dissipation of vorticity. Linearize about a mean zonal flow to give

$$\frac{\partial \zeta'}{\partial t} + \bar{u} \frac{\partial \zeta'}{\partial x} + \gamma v' = F'_\zeta - D'_\zeta, \quad (15.23)$$

where

$$\gamma = \beta - \frac{\partial^2 \bar{u}}{\partial y^2} \quad (15.24)$$

is the meridional gradient of absolute vorticity. (We use  $\gamma$  rather than  $\beta^*$  to denote this quantity because the argument may be extended to layered models, where  $\gamma = \partial \bar{q} / \partial y$ .) Now multiply (15.23) by  $\zeta' / \gamma$  and zonally average, assuming that  $\bar{u}_{yy}$  is small compared to  $\beta$  or varies only slowly, to form the pseudomomentum equation,

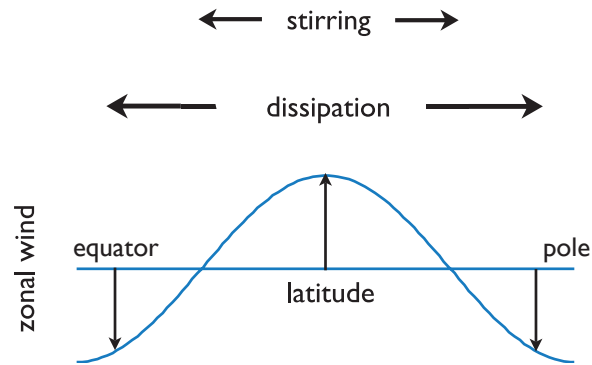
$$\frac{\partial \mathcal{P}}{\partial t} + \overline{v'\zeta'} = \frac{1}{\gamma} (\overline{\zeta' F'_\zeta} - \overline{\zeta' D'_\zeta}), \quad (15.25)$$

where

$$\mathcal{P} = \frac{1}{2\gamma} \overline{\zeta'^2} \quad (15.26)$$



**Fig. 15.5** Mean flow generation by a meridionally confined stirring. Because of Rossby wave propagation away from the source region, the distribution of pseudomomentum dissipation is broader than that of pseudomomentum forcing, and the sum of the two leads to the zonal wind distribution shown, with positive (eastward) values in the region of the stirring. See also Fig. 15.8.



is a wave activity density, equal to the pseudomomentum for this problem (see Section 10.2 and (10.29b) for related discussion). The parameter  $\gamma$  is positive if the average absolute vorticity increases monotonically northward, and this is usually the case in both Northern and Southern Hemispheres.

In the absence of forcing and dissipation, (15.21) and (15.25) imply an important relationship between the change of the mean flow and the pseudomomentum, namely

$$\frac{\partial \bar{u}}{\partial t} + \frac{\partial \mathcal{P}}{\partial t} = 0. \quad (15.27)$$

Now if for some reason  $\mathcal{P}$  increases, perhaps because a wave enters an initially quiescent region because of stirring elsewhere, then mean flow must decrease. However, because the vorticity flux integrates to zero, the zonal flow cannot decrease everywhere. Thus, if the zonal flow decreases in regions away from the stirring, it must *increase* in the region of the stirring. In the presence of forcing and dissipation this mechanism can lead to the production of a statistically steady jet in the region of the forcing, since (15.21) and (15.25) combine to give

$$\frac{\partial \bar{u}}{\partial t} + \frac{\partial \mathcal{P}}{\partial t} = -r\bar{u} + \frac{1}{\gamma} (\overline{\zeta' F'_\zeta} - \overline{\zeta' D'_\zeta}), \quad (15.28)$$

and in a statistically steady state

$$r\bar{u} = \frac{1}{\gamma} (\overline{\zeta' F'_\zeta} - \overline{\zeta' D'_\zeta}). \quad (15.29)$$

The terms on the right-hand side represent the stirring and dissipation of vorticity, and integrated over latitude their sum will vanish, or otherwise the pseudomomentum budget cannot be in a steady state. However, let us suppose that forcing is confined to mid-latitudes. In the forcing region, the first term on the right-hand side of (15.29) will be larger than the second, and an eastward mean flow will be generated. Away from the direct influence of the forcing, the dissipation term will dominate and westward mean flows will be generated, as sketched in Fig. 15.5. Thus, *on a  $\beta$ -plane or on the surface of a rotating sphere an eastward mean zonal flow can be maintained by a vorticity stirring that imparts no net momentum to the fluid.* In general, stirring in the presence of a vorticity gradient will give rise to a mean flow, and on a spherical planet the vorticity gradient is provided by differential rotation.

It is crucial to the generation of a mean flow that the dissipation has a broader latitudinal distribution than the forcing: if all the dissipation occurred in the region of the forcing then from (15.29) no mean flow would be generated. This broadening arises via the action of Rossby waves that are generated in the forcing region and that propagate meridionally before dissipating, as described in the previous subsection, so allowing the generation of a mean flow.



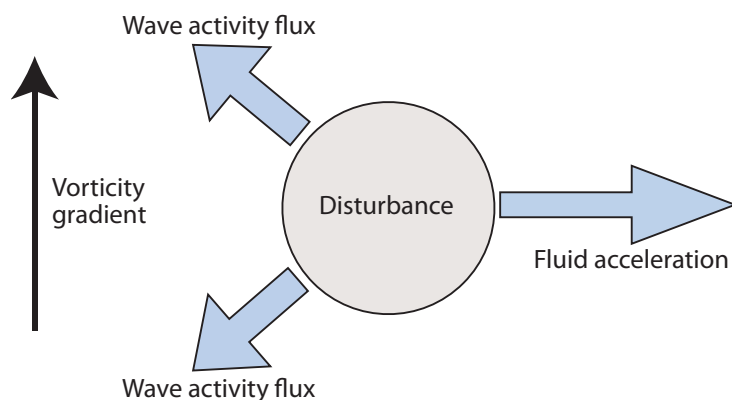


**Fig. 15.6** If a region of fluid on the  $\beta$ -plane or on a rotating sphere is stirred, then Rossby waves propagate away from the disturbance, and this is the direction of the wave-activity flux vector. Thus, there is divergence of wave activity in the stirred region, and using (15.34) this produces an eastward acceleration.

#### IV. The Eliassen–Palm flux

The Eliassen–Palm (EP) flux (Section 10.2) provides a convenient framework for determining how waves affect the mean flow, and the barotropic case is a particularly simple and instructive example. In the unforced case, the zonally-averaged momentum equation may be written as

$$\frac{\partial \bar{u}}{\partial t} - f_0 \bar{v}^* = \nabla_x \cdot \mathcal{F}, \quad (15.30)$$

where  $\bar{v}^*$  is the residual meridional velocity and  $\mathcal{F}$  is the Eliassen–Palm flux, and  $\nabla_x \cdot$  is the divergence in the meridional plane. In the barotropic case  $\bar{v}^* = 0$  and

$$\mathcal{F} = -\mathbf{j} \overline{u'v'}. \quad (15.31)$$

If the momentum flux is primarily the result of interacting nearly monochromatic waves, then the EP flux obeys the group velocity property (Section 6.7), namely that the flux of wave activity density is equal to the group velocity multiplied by the wave activity density. Thus,

$$\mathcal{F}^y \equiv \mathbf{j} \cdot \mathcal{F} \approx c_g^y \mathcal{P}, \quad (15.32)$$

where  $\mathcal{P}$  is the wave activity density, or pseudomomentum, given by

$$\mathcal{P} = \frac{\overline{\zeta'^2}}{2\bar{q}_y} = \frac{\overline{\zeta'^2}}{2\gamma}, \quad (15.33)$$

and, if  $\gamma > 0$ ,  $\mathcal{P}$  is a positive-definite quantity. The zonal momentum equation and the Eliassen–Palm relation (10.29a) become respectively

$$\frac{\partial \bar{u}}{\partial t} = \frac{\partial}{\partial y} (c_g^y \mathcal{P}), \quad \frac{\partial \mathcal{P}}{\partial t} + \frac{\partial}{\partial y} (c_g^y \mathcal{P}) = 0, \quad (15.34a,b)$$

and so

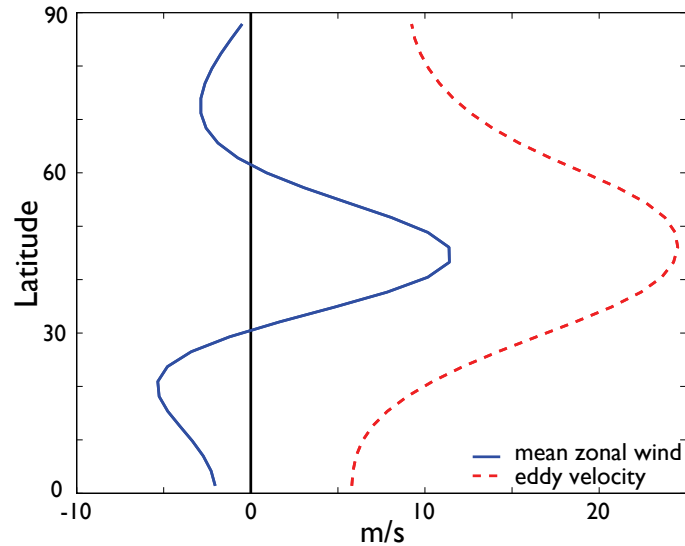
$$\frac{\partial \bar{u}}{\partial t} = -\frac{\partial \mathcal{P}}{\partial t}, \quad (15.35)$$

as in (15.27).

Now suppose that we initiate a disturbance at some latitude, and then let the fluid evolve freely. The disturbance generates Rossby waves whose group velocity will be directed away from the region of disturbance, and from (15.34b) the wave activity density  $\mathcal{P}$  will diminish in the region of

**Fig. 15.7** The time and zonally-averaged wind (solid line) obtained by an integration of the barotropic vorticity equation (15.36) on the sphere.

The fluid is stirred in mid-latitudes by a random wavemaker that is statistically zonally uniform, acting around zonal wavenumber 8, and that supplies no net momentum. Momentum converges in the stirring region leading to an eastward jet with a westward flow to either side, and zero area-weighted spatially integrated velocity. The dashed line shows the r.m.s. (eddy) velocity created by the stirring.



the disturbance (and increase elsewhere). However, from (15.34a) the zonal velocity will *increase* in the region of the disturbance, and an eastward flow will be generated. That is, momentum converges in the region of the disturbance and an eastward jet is generated, as sketched in Fig. 15.6.

The EP flux argument, the pseudomomentum argument and the Rossby wave argument are just different expressions of the same physical process. Indeed, the result of (15.10) can be regarded as illustrating the group velocity property of the EP flux for barotropic Rossby waves. The vorticity budget argument is a little more general than these arguments, because it does not depend on linearization or small amplitude disturbances. None of these arguments requires that the flow be truly turbulent and, although they all involve nonlinear interactions, it is the presence of the  $\beta$ -effect — a linear term in the vorticity equation — that is crucial in the development of a mean flow.

### 15.1.3 A Numerical Example

We conclude from the above arguments that momentum will converge into a rapidly rotating flow that is stirred in a meridionally localized region. To illustrate this, we numerically integrate the barotropic vorticity equation on the sphere, with a meridionally localized stirring term; explicitly, the equation that is integrated is

$$\frac{\partial \zeta}{\partial t} + J(\psi, \zeta) + \beta \frac{\partial \psi}{\partial x} = -r\zeta + \kappa \nabla^4 \zeta + F_\zeta. \quad (15.36)$$

The first term on the right-hand side is a linear drag, parameterizing momentum loss in an Ekman layer. The second term removes enstrophy that has cascaded to small scales; it has a negligible impact at large scales. The forcing term  $F_\zeta$  is a wavemaker confined to a zonal strip of about  $15^\circ$  meridional extent, centred at about  $45^\circ$  N, that is statistically zonally uniform and that spatially integrates to zero. Within that region it is a random stirring with a temporal decorrelation scale of a few days and a spatial decorrelation scale corresponding to about wavenumber 8, thus mimicking weather scales. Thus, it provides no net source of vorticity or momentum, but it is a source of pseudomomentum because  $\overline{F_\zeta \zeta} > 0$ .

The results of a numerical integration of (15.36) are illustrated in Figs. 15.7 and 15.8. An eastward jet forms in the vicinity of the forcing, with westward flow on either side. The pseudomomentum stirring and dissipation that produce this flow are shown in Fig. 15.8. As expected, the

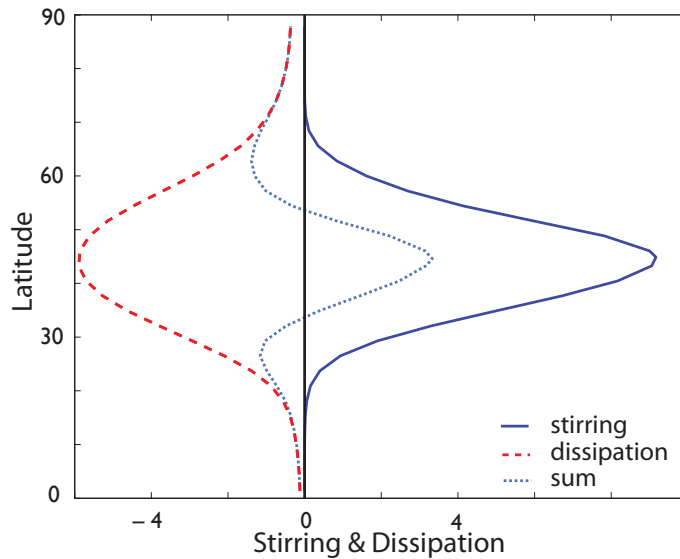


**Fig. 15.8** The pseudomomentum stirring (solid line,  $\overline{F}_\zeta' \zeta'$ ), dissipation (red dashed line,  $\overline{D}_\zeta' \zeta'$ ) and their sum (dotted), for the same integration as Fig. 15.7.

Because Rossby waves propagate away from the stirred region before breaking, the distribution of dissipation is broader than the forcing, resulting in an eastward jet where the stirring is centred, with westward flow on either side.

dissipation has a broader distribution than the forcing, and the sum of the two (the dotted line) has the same meridional distribution as the zonal flow itself.

## 15.2 LAYERED MODELS OF THE MID-LATITUDE CIRCULATION

Let us now extend our barotropic model in the direction of increasing realism. So far we have shown that localized stirring can give rise to an eastward acceleration as Rossby waves propagate away from the disturbance. The source of the disturbance is baroclinic instability, and to incorporate that effects will necessitate some vertical structure into the problem; we do this by way of layered models of the circulation.<sup>4</sup> That is, we consider an atmosphere to consist of one or more isentropic layers, as described in Section 3.10. The equations describing such layers are virtually isomorphic to the shallow water equations and, for the sake of familiarity and simplicity, and with no loss of essential dynamics, we use the Boussinesq shallow water equations. We begin with a model of a single layer, with summaries for the impatient on page 552 and on page 556.

### 15.2.1 A Single-layer Model

We first consider a single layer obeying the shallow water equations. We further restrict the flow by supposing that it is constrained by two rigid surfaces: an upper flat lid and a lower, wavy (but stationary) surface (Fig. 15.9). We may imagine the fluid layer to crudely represent the upper troposphere, with the (given) lower wavy surface corresponding to the undulating mid-atmosphere interface of a two-layer model. (This section is in some ways an exercise, and too much realism should not be ascribed to the model.) Thus frictional effects are small in the momentum equation, and in particular there is no Ekman layer and no drag on the velocity field. However, there may be some dissipative effects in the vorticity equation, arising from the cascade of enstrophy to small scales. We also suppose that the Rossby number is small, that the variations in layer thickness are small compared to the mean layer thickness, and that variations in Coriolis parameter are small. Let the initial flow be a uniform zonal current, passing over the wavy lower boundary. The boundary is waviest in mid-latitudes, creating a disturbance from which Rossby waves emanate. Our questions are: (i) How does the wavy interface affect the mean zonal flow? (ii) What if any meridional circulation is induced?

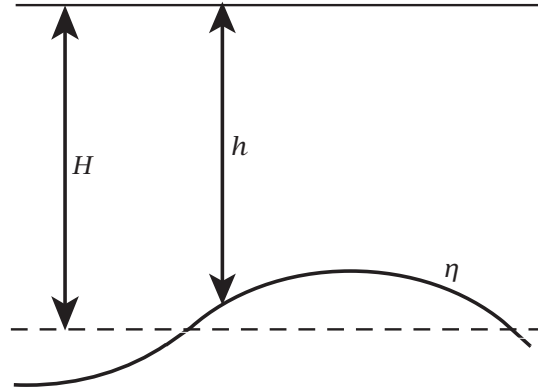


**Fig. 15.9** A model atmosphere with an active layer of mean thickness  $H$ , local thickness  $h$ , and a variable lower surface of height displacement  $\eta$ , lying above a stationary layer with a slightly larger potential density.

### Equations of motion

The zonal momentum equation for the layer may be written as

$$\frac{\partial u}{\partial t} - (f + \zeta)v = -\frac{\partial B}{\partial x}, \quad (15.37)$$

where  $B = \phi + u^2/2$  is the Bernoulli function for the problem and  $\phi$  is the kinematic pressure,  $p/\rho_0$ . The zonal average of the equation is

$$\frac{\partial \bar{u}}{\partial t} - f\bar{v} = \bar{\zeta}\bar{v} + \overline{\zeta'v'}. \quad (15.38)$$

Note that  $\bar{v}$  is wholly ageostrophic ( $\bar{v}_g = \partial_x \bar{\psi} = 0$ ). Now, using  $\partial u/\partial x + \partial v/\partial y = 0$ , the vorticity flux is related to the momentum flux by

$$v\zeta = -\frac{\partial}{\partial y}(uv) + \frac{1}{2}\frac{\partial}{\partial x}(v^2 - u^2), \quad (15.39)$$

so that, under quasi-geostrophic scaling, (15.38) simplifies to

$$\frac{\partial \bar{u}}{\partial t} - f_0\bar{v} = \overline{\zeta'v'} = -\frac{\partial}{\partial y}\overline{u'v'}. \quad (15.40)$$

Although  $\bar{v}$  is small and ageostrophic, mass conservation does not demand that it be zero, because the thickness of the layer is not constant — look ahead to (15.43). Thus, as  $\bar{v}$  is multiplied by the large term  $f_0$ , the term  $f_0\bar{v}$  term should be retained (whereas  $\bar{\zeta}\bar{v}$  is dropped). If the flow is statistically steady and there are no sources or sinks of momentum (15.40) becomes

$$f_0\bar{v} = \frac{\partial}{\partial y}\overline{u'v'}. \quad (15.41)$$

To complete the model we use the zonally-averaged mass conservation equation, namely

$$\frac{\partial \bar{h}}{\partial t} + \frac{\partial}{\partial y}\overline{vh} = 0. \quad (15.42)$$

In the situation here  $\partial \bar{h}/\partial t = 0$ , because the flow is confined between two rigid surfaces, and so  $\partial \bar{v}h/\partial y = 0$ . If the mass flux vanishes somewhere, for example at a meridional boundary, it therefore vanishes everywhere and we have

$$\bar{v}\bar{h} + \overline{v'h'} = 0. \quad (15.43)$$

Using (15.41) and (15.43) gives

$$\frac{1}{f_0} \frac{\partial}{\partial y} \overline{u'v'} + \frac{\overline{v'h'}}{h} = 0, \quad \text{or} \quad \overline{v'\zeta'} - f_0 \frac{\overline{v'h'}}{h} = 0. \quad (15.44a,b)$$

Because thickness variations are assumed to be small we may write this as

$$\overline{v'\zeta'} - f_0 \frac{1}{H} \overline{v'h'} = 0, \quad (15.45)$$

where  $H$  is the reference thickness of the layer, which may be taken as its mean thickness. The left-hand side of (15.45) is actually just the potential vorticity flux for this problem — look ahead to (15.51). The potential vorticity equation for the layer is

$$\frac{DQ}{Dt} = \frac{D}{Dt} \left[ \frac{\zeta + f}{h} \right] = 0, \quad (15.46)$$

where  $h$  is the fluid layer thickness. For small variations in layer thickness and Coriolis parameter this becomes

$$\frac{Dq}{Dt} = \frac{\partial q}{\partial t} + u \frac{\partial q}{\partial x} + v \frac{\partial q}{\partial y} = 0, \quad q = \zeta + \beta y + f_0 \frac{\eta}{H}, \quad (15.47a,b)$$

where  $\eta = H - h$  is the height of the lower interface (Fig. 15.9) and this is a function of  $x$  and  $y$  but not, in this model, time. Using the horizontal non-divergence of the flow, the zonally-averaged potential vorticity equation is

$$\frac{\partial \bar{q}}{\partial t} = -\frac{\partial \bar{v} \bar{q}}{\partial y} - \frac{\partial \overline{v'q'}}{\partial y}. \quad (15.48)$$

The term involving  $\bar{v}$  is very small, and omitting it and using (15.47a) we obtain the perturbation potential vorticity equation

$$\frac{\partial q'}{\partial t} + \bar{u} \frac{\partial q'}{\partial x} + v' \frac{\partial \bar{q}}{\partial y} = -D', \quad (15.49)$$

where we include a term,  $D'$ , to represent dissipative processes. Multiplying by  $q' / (\partial \bar{q} / \partial y)$  and zonally averaging we obtain the pseudomomentum equation for this system, namely

$$\frac{\partial \mathcal{P}}{\partial t} = \frac{\partial}{\partial t} \left( \frac{\overline{q'^2}}{2\gamma} \right) = -\overline{v'q'} - \frac{\overline{D'q'}}{\gamma}, \quad (15.50)$$

where  $\gamma = \partial \bar{q} / \partial y$ . This equation is the equivalent of (15.25), but now for the layered system. In a turbulent fluid we cannot, in general, demand that  $D' = 0$ , even as the viscosity goes to zero, because of the presence of an enstrophy flux to smaller scales and a concomitant dissipation. But in regions where  $D'$  is zero (where there is no wave breaking) then the potential vorticity flux must also be zero in a steady state. For our argument let us assume that, in fact,  $D' = 0$ .

Using (15.47b), the eddy potential vorticity flux is

$$\overline{v'q'} = \overline{v'\zeta'} + \frac{f_0}{H} \overline{v'\eta'} = \overline{v'\zeta'} - \frac{f_0}{H} \overline{v'h'}, \quad (15.51)$$

where  $\eta'$  is the topography and  $h'$  is the layer thickness perturbation. Using this in the zonal momentum equation (15.40) gives

$$\frac{\partial \bar{u}}{\partial t} = \overline{v'q'} + \frac{f_0}{H} \overline{v'h'} + f_0 \bar{v}. \quad (15.52)$$

### Informal Summary of the Single-layer Arguments

The zonally-averaged momentum equation is

$$\frac{\partial \bar{u}}{\partial t} - f_0 \bar{v} = \overline{v' \zeta'} = -\frac{\partial \overline{u' v'}}{\partial y}. \quad (\text{SL.1})$$

A region that is the source of Rossby waves will generally be a region where there is momentum flux convergence, where  $\partial \overline{u' v'} / \partial y < 0$ . In this region  $\bar{v}$  will be directed *equatorward* if  $\bar{u}$  is steady, and this flow is the upper branch of the Ferrel Cell. To think about this in terms of potential vorticity, first define the residual meridional velocity by

$$\bar{v}^* = \frac{\overline{v' h'}}{\bar{h}} + \bar{v}. \quad (\text{SL.2})$$

This is proportional to the total meridional mass flux in a layer, and is zero in this one-layer model. The momentum equation is then

$$\frac{\partial \bar{u}}{\partial t} = f_0 \bar{v}^* - \frac{f_0}{\bar{h}} \overline{v' h'} + \overline{v' \zeta'} \quad (\text{SL.3a})$$

$$= f_0 \bar{v}^* + \overline{v' q'}. \quad (\text{SL.3b})$$

using  $\overline{v' q'} = \overline{v' \zeta'} - (f_0 / \bar{h}) \overline{v' h'}$ , where  $q$  is the potential vorticity. The second term on the right-hand side of (SL.3a) is the *form drag* exerted by the topography on the flow, and in a steady state this balances the momentum flux convergence of the Rossby waves. Because of the presence of Rossby waves we expect  $\overline{v' \zeta'} > 0$ . If there is no dissipation then in steady flow  $\overline{v' q'} = -f_0 \bar{v}^* = 0$  and the eddy mass flux is poleward (positive if  $f_0 > 0$ ) and a meridional flow is generated as in Fig. 15.10.

We can infer the potential vorticity flux more directly using the pseudomomentum equation:

$$\frac{\partial \mathcal{P}}{\partial t} = \frac{\partial}{\partial t} \left( \frac{\overline{q'^2}}{2\gamma} \right) = -\overline{v' q'} - \frac{\overline{D' q'}}{\gamma}, \quad (\text{SL.4})$$

where  $\gamma = \partial \bar{q} / \partial y$ . If dissipation is identically zero, then the potential vorticity flux is zero if the waves are steady. Then, using (SL.3b), there is no acceleration of the zonal flow — an example of the *non-acceleration theorem*.

More generally (and in the real atmosphere) there *will* be some dissipation away from the source region: Rossby waves will preferentially break in critical layers (near where  $\bar{u} = c$ ) and/or more generally Rossby waves will interact producing an enstrophy cascade. These processes give  $\overline{D' q'} > 0$  and (for  $\gamma > 0$ ) a negative potential vorticity flux,  $\overline{v' q'} < 0$ . In these regions, a balance in the momentum equation (SL.3b) can be achieved either by balancing the PV flux with a friction term, as in the barotropic model of Section 15.1, or by a Coriolis force on a poleward residual meridional velocity. That is,  $f_0 \bar{v}^* \approx -\overline{v' q'} > 0$ , so generating a poleward residual flow.

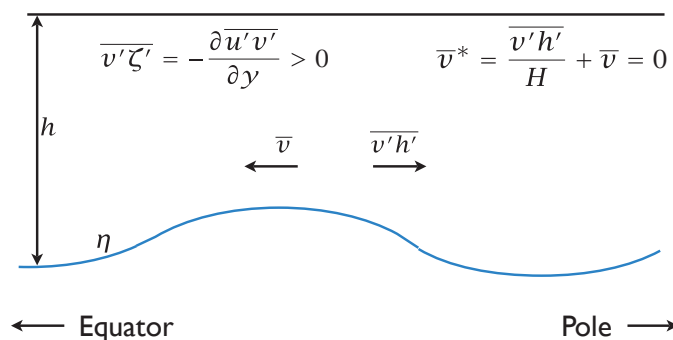


**Fig. 15.10** Dynamics of a single layer, with no dissipation. The force on the active layer arises from the form drag exerted by the interface. Vorticity dynamics demands that this produce a converging eddy momentum flux ( $\partial_y \overline{u'v'} < 0$ ), which in turn produces a poleward eddy mass flux ( $\overline{v'h'} > 0$ ), and so an equatorward Eulerian flow.

But the last two terms on the right-hand side constitute the total mass flux, so we finally write

$$\frac{\partial \bar{u}}{\partial t} = \overline{v'q'} + f_0 \bar{v}^*, \quad \bar{v}^* = \bar{v} + \frac{\overline{v'h'}}{H}. \quad (15.53a,b)$$

The quantity  $\bar{v}^*$  is the *residual circulation* for this problem; it is proportional to the sum of mass flux from the mean flow and the eddies (see Section 10.3 for more discussion). Now,  $\bar{v}^*$  is proportional to the total meridional mass flux and therefore here, because the flow is confined between rigid lids and if there are no sources or sinks of mass,  $\bar{v}^* = 0$  everywhere (see (15.43) with  $\bar{h} = H$ ).

### Dynamics

When the flow passes over the wavy boundary, Rossby waves will, as in the barotropic case, cause momentum flux to converge in the generation region. If the flow is steady and dissipation-free then from the momentum equation

$$f_0 \bar{v} = \frac{\partial \overline{u'v'}}{\partial y}, \quad (15.54)$$

and, in regions of momentum flux convergence (i.e., where  $\partial \overline{u'v'}/\partial y < 0$ ) the mean meridional velocity is equatorward. Thus, whereas frictional forces balance the vorticity flux in a constant-thickness barotropic model (because in that case  $\bar{v} = 0$ ) in the free atmosphere a meridional circulation may be generated, and this is the basis of the equatorial flow in the upward branch of the Ferrel cell. However, this does not imply that the total mass flux is equatorward; in fact, for this single-layer model it must be zero, and therefore

$$\overline{v'h'} = -\bar{h}\bar{v} > 0. \quad (15.55)$$

That is, the eddy mass flux is poleward, balancing the equatorward mean flow. These balances are sketched in Fig. 15.10.

Another way to arrive at this result is to utilize potential vorticity fluxes directly. For steady, dissipation-free flow the pseudomomentum equation (15.50) reveals that the potential vorticity flux vanishes. Then using (15.53) and noting that  $\bar{v}^* = 0$  we have  $\partial \bar{u}/\partial t = 0$  — an example of the non-acceleration theorem that steady non-dissipative waves do not induce a change in the zonal momentum. Then, using (15.51) we find

$$\overline{v'\zeta'} = \frac{f_0}{H} \overline{v'h'}, \quad (15.56)$$

and using (15.43) we recover (15.54).



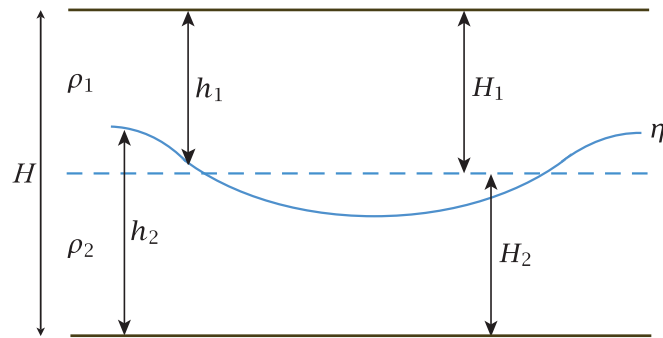


**Fig. 15.11** An atmosphere with two homogeneous (or isentropic) layers of mean thickness  $H_1$  and  $H_2$ , local thickness  $h_1$  and  $h_2$ , and interface  $\eta$ , contained between two flat, rigid surfaces.

From the point of view of the momentum equation, the momentum flux convergence is balanced by the *form drag* caused by the flow over the wavy boundary. To see this we use (15.53b) to write the zonal momentum equation as

$$\frac{\partial \bar{u}}{\partial t} = f_0 \bar{v} + \overline{v' \zeta'} = f_0 \bar{v}^* - \frac{f_0}{H} \overline{v' h'} + \overline{v' \zeta'}, \quad (15.57)$$

where here  $\bar{v}^*$  (but not  $\bar{v}$ ) is zero. The term  $-(f_0/H) \overline{v' h'}$  represents the force on the fluid layer coming from the wavy boundary — the form drag, as described in Section 3.6. Specifically, the average force per unit area exerted on the layer by the sloping surface is given by

$$F = -f_0 \rho_0 \overline{v' \eta'} = f_0 \rho_0 \overline{v' h'}, \quad (15.58)$$

and dividing by  $\rho_0 H$  provides the acceleration on the active fluid layer. The atmosphere also exerts an equal and opposite force on the wavy surface, an effect we consider in the next section. A steady state is achieved, without dissipation, when the form drag is balanced by the eddy momentum flux convergence. From (15.51) or (15.53), this state is the same as the condition that the potential vorticity flux vanishes.

#### Final remarks on the one-layer model

A summary of the single-layer arguments is given in the shaded box on page 552. In the single-layer model, as in the barotropic model, the zonal flow is proximately driven by eddy fluxes of potential vorticity, and in the model the eddy fluxes must be zero if a steady state is to be achieved. *Vis-à-vis* the real atmosphere this is a little unrealistic, because from the pseudomomentum equation (15.50) we expect these fluxes to be negative, and there is then nothing to balance them in the momentum equation, (15.53), if  $\bar{v}^* = 0$ . In the real atmosphere, there are effectively sources and sinks in the mass conservation equation that arise from the thermodynamics that allow  $\bar{v}^*$  to be non-zero; we then expect  $\bar{v}^* > 0$ , but to explore this requires a two-layer model, in which the single layer of the one-layer model will correspond to the upper layer of the two-layer model.

### 15.2.2 A Two-layer Model

We now consider a model with two active layers, constructing what is probably the simplest model that can capture the dynamics of the mid-latitude tropospheric general circulation without undue approximation. Indeed virtually all of the phenomenology that we associate with the circulation — a thermal wind, mid-latitude surface westerly winds, the Ferrel cell, breaking Rossby waves — is present. A three-layer model introduces no new physics, although a continuously stratified model does lead to some differences of interpretation. The physical model we have in mind is one of two isentropic layers of a compressible ideal gas, virtually equivalent to a two-layer shallow water model illustrated in Fig. 15.11, and our presentation will be in terms of the latter. The upper layer

may be thought of as being forced by an undulating interface between the lower and upper layers, a crude representation of stratification. We continue to assume that quasi-geostrophic scaling holds; that is, the flow is in near geostrophic balance, variations in layer thickness are small compared to their mean thickness and variations in the Coriolis parameter are small. We also assume that the two fluid layers are held between two flat rigid lids — topography is an unnecessary complication at this stage.

### Equations of motion

The equations of motion are those of a two-layer Boussinesq shallow water model confined between two rigid flat surfaces, and readers comfortable with these dynamics (see Sections 3.3 and 3.5) may quickly skip through this section, glancing at the boxed equations, and look at the summary on the next page. The momentum equations of each layer are

$$\frac{D\mathbf{u}_1}{Dt} + \mathbf{f} \times \mathbf{u}_1 = -\nabla\phi_1, \quad (15.59a)$$

$$\frac{D\mathbf{u}_2}{Dt} + \mathbf{f} \times \mathbf{u}_2 = -\nabla\phi_2 - r\mathbf{u}_2, \quad (15.59b)$$

where  $\phi_1 = p_T/\rho_0$  and  $\phi_2 = p_T/\rho_0 + g'\eta$ , with  $p_T$  being the pressure at the lid at the top,  $\eta$  the interface displacement (see Fig. 15.11) and  $g' = g(\rho_2 - \rho_1)/\rho_0$  the reduced gravity, and we may take  $\rho_0 = \rho_1$ . We have also included a simple representation of surface drag,  $-r\mathbf{u}_2$ , in the lowest layer, and  $r$  is a constant. We will use a constant value of the Coriolis parameter except where it is differentiated, and on zonal averaging the zonal components of (15.59) become

$$\frac{\partial \bar{u}_1}{\partial t} - f_0 \bar{v}_1 = \overline{v'_1 \zeta'_1} \quad (15.60a)$$

$$\frac{\partial \bar{u}_2}{\partial t} - f_0 \bar{v}_2 = \overline{v'_2 \zeta'_2} - r \bar{u}_2. \quad (15.60b)$$

Geostrophic balance in each layer implies

$$f_0 \mathbf{u}_{g1} = \mathbf{k} \times \nabla\phi_1, \quad f_0 \mathbf{u}_{g2} = \mathbf{k} \times \nabla\phi_1 + g' \mathbf{k} \times \nabla\eta, \quad (15.61a,b)$$

where the subscript  $g$  denotes geostrophic. Subtracting one equation from the other gives

$$f_0(\mathbf{u}_1 - \mathbf{u}_2) = -g' \mathbf{k} \times \nabla\eta, \quad (15.62)$$

dropping the subscripts  $g$  on  $\mathbf{u}$ . This equation represents thermal wind balance (or the Margules relation) for this system. A temperature gradient thus corresponds to a slope of the interface height, with the interface sloping upwards toward lower temperatures, analogous to isentropes sloping up toward the pole in the real atmosphere.

The quasi-geostrophic potential vorticity for each layer is

$$q_i = \zeta_i + f - f_0 \frac{h_i}{H_i}, \quad (15.63)$$

where  $H_i$  is the reference thickness of each layer, which we take to be its mean thickness. The potential vorticity flux in each layer is then

$$\overline{v'_i q'_i} = \overline{v'_i \zeta'_i} - \frac{f_0}{H_i} \overline{v'_i h'_i}. \quad (15.64)$$

### Phenomenology of a Two-layer Mid-Latitude Atmosphere

A radiative forcing that heats low latitudes and cools high latitudes will lead to an isentropic interface that slopes upward with increasing latitude, and a poleward total mass flux in the upper layer and an equatorward flux in the lower layer. The interface implies a thermal wind shear between the two layers. Neglecting relative vorticity, the potential vorticity gradients in each layer are given by

$$\frac{\partial \bar{q}_1}{\partial y} = \beta - \frac{f_0}{H_1} \frac{\partial \bar{h}_1}{\partial y} > 0 \quad \text{and} \quad \frac{\partial \bar{q}_2}{\partial y} = \beta - \frac{f_0}{H_2} \frac{\partial \bar{h}_2}{\partial y} \lesssim 0. \quad (\text{TL.1})$$

The gradient generally is large and positive in the upper layer and small and negative in the lower layer — the gradient must change sign if there is to be baroclinic instability as we assume to be the case. This baroclinic instability generates eddy fluxes that largely determine the surface winds and the meridional overturning circulation. The zonal momentum equation in each layer is

$$\frac{\partial \bar{u}_1}{\partial t} = f_0 \bar{v}_1 + \overline{v'_1 \zeta'_1} = f_0 \bar{v}_1^* + \overline{v'_1 q'_1}, \quad (\text{TL.2a})$$

$$\frac{\partial \bar{u}_2}{\partial t} = f_0 \bar{v}_2 + \overline{v'_2 \zeta'_2} - r \bar{u}_2 = f_0 \bar{v}_2^* + \overline{v'_2 q'_2} - r \bar{u}_2, \quad (\text{TL.2b})$$

where

$$\bar{v}_i^* = \bar{v}_i + \frac{\overline{v'_i h'_i}}{H_i} \quad (\text{TL.3})$$

is the residual meridional flow. In steady state the potential vorticity flux will be equatorward in the upper layer and poleward in the lower layer. Because the mass flux in each layer is equal and opposite, the surface (i.e., lower-layer) wind is given by the vertical integral of the vorticity or potential vorticity fluxes, namely

$$r H_2 \bar{u}_2 = H_1 \overline{v'_1 q'_1} + H_2 \overline{v'_2 q'_2} = H_1 \overline{v'_1 \zeta'_1} + H_2 \overline{v'_2 \zeta'_2}. \quad (\text{TL.4})$$

The vorticity flux is positive in the upper layer and negative in the lower layer. However, because the potential vorticity gradient in the upper layer is large, this layer is more linear than the lower layer and Rossby waves are better able to transport momentum. The magnitude of the vorticity flux is thus larger in the upper layer than in the lower layer and, using (TL.4), the surface winds are positive (eastward) in the mid-latitude baroclinic zone (see Fig. 15.14).

To balance the upper-layer mid-latitude momentum flux convergence a meridional overturning circulation (a Ferrel cell) is generated. In a steady state  $f_0 \bar{v}_1 = -\overline{v'_1 \zeta'_1}$  so that the zonally-averaged upper level flow is equatorward. However, the total mass flux in the upper level is poleward; thus, the equatorward meridional velocity in the upper branch of the Ferrel cell is the consequence of an Eulerian zonal average and does not correspond to a net equatorward mass transport.

In the real atmosphere, the equatorward residual flow occurs close to the surface. Thus, for more realism, we might think of the lower layer as representing a near-surface layer and choose  $H_1 \gg H_2$ , or even construct a three-layer model with a shallow near-surface layer and two interior layers.

Using this in (15.60) gives

$$\frac{\partial \bar{u}_1}{\partial t} = \overline{v'_1 q'_1} + f_0 \bar{v}_1^*, \quad \frac{\partial \bar{u}_2}{\partial t} = \overline{v'_2 q'_2} + f_0 \bar{v}_2^* - r \bar{u}_2, \quad (15.65a,b)$$

where

$$\bar{v}_i^* = \bar{v}_i + \frac{\overline{v'_i h'_i}}{H_i} \quad (15.66)$$

is the meridional component of the residual velocity in each layer, proportional to the *total* meridional mass flux in each layer. These are the transformed Eulerian mean (TEM) forms of the equations, first encountered in Section 10.3.

In the barotropic model of Section 15.1 the mean meridional velocity vanished at every latitude, a consequence of mass conservation in a single layer between two rigid flat surfaces. In the single-layer model of Section 15.2.1 the mean meridional velocity was in general non-zero, but the total meridional mass flux (i.e., the meridional component of the residual velocity) was zero if the domain is bounded laterally by solid walls. In the two-layer model we will allow a transformation of mass from one layer to another, which is the equivalent of heating: a conversion of mass from the lower layer to the upper layer is heating, and conversely for cooling. Thus, heating at low latitudes and cooling at high latitudes leads to the interface sloping upwards toward the pole. In the two-layer model the constraint that mass conservation supplies is that, assuming a statistically steady state, the total poleward mass flux summed over both layers must vanish.

The mass conservation equation for each layer is

$$\frac{\partial h_i}{\partial t} + \nabla \cdot (h_i \mathbf{u}_i) = S_i, \quad (15.67)$$

where  $S_i$  is the mass source term and we may suppose that  $S_1 + S_2 = 0$  everywhere. A zonal average gives

$$\frac{\partial \bar{h}_i}{\partial t} + \frac{\partial \bar{h}_i \bar{v}_i}{\partial y} = \bar{S}_i, \quad (15.68)$$

or, setting  $\bar{h}_i = H_i$  and using (15.66),

$$\frac{\partial \bar{h}_i}{\partial t} + H_i \frac{\partial \bar{v}_i^*}{\partial y} = \bar{S}_i. \quad (15.69)$$

The mass source term in these equations is equivalent to heating, and let us suppose that this is such as to provide heating at low latitudes and cooling at high ones. This is equivalent to conversion of an upper-layer mass to a lower-layer mass at high latitudes, and the reverse at low latitudes; such a conversion can only be balanced by a poleward mass flux in the upper layer and an equatorward mass flux in the lower layer (Fig. 15.12). That is to say, an Earth-like radiative forcing between equator and pole implies that *the total mass flux in the upper layer will be poleward*. This is the opposite of the mean meridional circulation of the Ferrel cell shown in Fig. 14.3! What's going on? Before we can answer that, let us manipulate the equations of motion and obtain a couple of useful preliminary results.

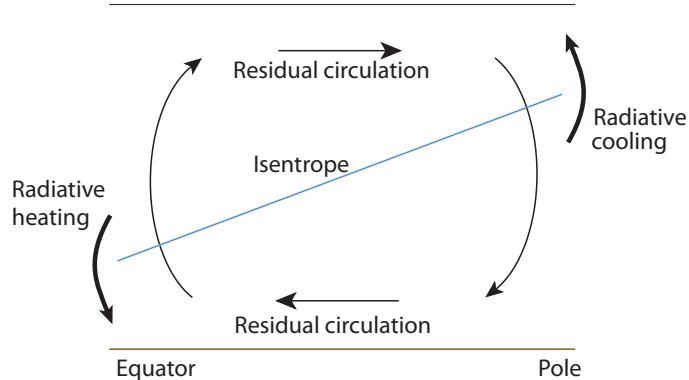
### Manipulating the equations

Because the total depth of the fluid is fixed, the mass conservation equations in each layer, (15.67), may each be written as an equation for the interface displacement, namely

$$\frac{\partial \eta}{\partial t} + \nabla \cdot (\eta \mathbf{u}_1) = -S_1, \quad \text{or} \quad \frac{\partial \eta}{\partial t} + \nabla \cdot (\eta \mathbf{u}_2) = S_2, \quad (15.70a,b)$$

**Fig. 15.12** Thermodynamics of a two-layer model, with an isentrope (or an interface between two layers) sloping up toward a cold pole, caused by cooling at high latitudes and heating at low.

The heating is balanced by a net mass flux — the meridional overturning circulation. In the tropics this circulation is the Hadley Cell, and is nearly all in the mean flow. In mid-latitudes the circulation is largely in the residual flow, and the Eulerian mean flow (the Ferrell Cell) is in the opposite sense.



where  $\eta = H_1 - h_1 = h_2 - H_2$  and  $h_1 + h_2 = H_1 + H_2$ . Because of the thermal wind equation, (15.62), (15.70a) and (15.70b) are identical:  $\mathbf{u}_1 \cdot \nabla \eta = \mathbf{u}_2 \cdot \nabla \eta$  and  $S_1 = -S_2$ . (If  $S_1 \neq -S_2$  the flow would not remain balanced and the thermal wind equation could not be satisfied.) The zonally-averaged interface equation may be written as

$$\frac{\partial \bar{\eta}}{\partial t} - H_1 \frac{\partial \bar{v}_1^*}{\partial y} = \bar{S}, \quad \text{or} \quad \frac{\partial \bar{\eta}}{\partial t} + H_2 \frac{\partial \bar{v}_2^*}{\partial y} = \bar{S}, \quad (15.71)$$

where  $\bar{S} = -\bar{S}_1 = +\bar{S}_2$ , consistent with the mass conservation statement

$$H_1 \bar{v}_1^* + H_2 \bar{v}_2^* = 0, \quad (15.72)$$

which states that the vertically integrated total mass flux vanishes at each latitude.

Now, whereas (15.72) is a kinematic statement about the total mass flux, the dynamics provides a constraint on the *eddy* mass flux in each layer. Using the thermal wind relationship we have

$$f_0 \overline{(v'_1 - v'_2)\eta'} = g' \frac{\partial \overline{\eta'}}{\partial x} \eta' = 0. \quad (15.73)$$

Hence, if the upper and lower surfaces are both flat, we have that

$$\overline{v'_1 h'_1} = -\overline{v'_2 h'_2}, \quad (15.74)$$

and the eddy meridional mass fluxes in each layer are equal and opposite. If the bounding surfaces are not flat, we have

$$\overline{v'_1 \eta'_T} - \overline{v'_1 h'_1} = \overline{v'_2 \eta'_B} + \overline{v'_2 h'_2} \quad (15.75)$$

instead, where  $\eta_T$  and  $\eta_B$  are the topographies at the top and the bottom. Equations (15.74) and (15.75) are *dynamical* results, and not just kinematic ones; they are equivalent to noting that the form drag on one layer due to the interface displacement is equal and opposite to that on the other, namely

$$\overline{v'_1 \eta'} = -[\overline{v'_2 \eta'}], \quad (15.76)$$

where the minus sign inside the square brackets arises because the interface displacement is into layer one but out of layer two.

Using (15.64) and (15.75) the eddy potential vorticity fluxes in the two layers are related by

$$H_1 \overline{v'_1 q'_1} + H_2 \overline{v'_2 q'_2} = H_1 \overline{v'_1 \zeta'_1} + H_2 \overline{v'_2 \zeta'_2} - f_0 \overline{v'_1 \eta'_T} + f_0 \overline{v'_2 \eta'_B}, \quad (15.77)$$

which is the layered version of the continuous result (see (10.26) on page 383),

$$\int_B^T \overline{v'q'} dz = \int_B^T \overline{v'\zeta'} dz + \frac{f_0}{N^2} [v'b']_B^T. \quad (15.78)$$

For flat upper and lower surfaces, and using  $\overline{v_i\zeta_i} = -\partial\overline{u_i v_i}/\partial y$ , (15.77) becomes

$$H_1 \overline{v'_1 q'_1} + H_2 \overline{v'_2 q'_2} = -H_1 \frac{\partial}{\partial y} \overline{u'_1 v'_1} - H_2 \frac{\partial}{\partial y} \overline{u'_2 v'_2}, \quad (15.79)$$

and integrating with respect to  $y$  between quiescent latitudes gives

$$\int [H_1 \overline{v'_1 q'_1} + H_2 \overline{v'_2 q'_2}] dy = 0. \quad (15.80)$$

That is, the total meridional flux of potential vorticity must vanish. This is a consequence of the fact that the potential vorticity flux is the divergence of a vector field; in the continuous case

$$\overline{v'q'} = -\frac{\partial \overline{u'v'}}{\partial y} + f_0 \frac{\partial}{\partial z} \frac{\overline{v'b'}}{N^2}, \quad (15.81)$$

which similarly vanishes when integrated over a volume if there are no boundary contributions.

### 15.2.3 Dynamics of the Two-layer Model

We now consider the climate, or the time averaged statistics, of our two-layer model. The equations of motion are (15.60) or (15.65), and (15.68) or (15.69). These equations are not closed because of the presence of eddy fluxes, and in this section we make some phenomenological and rather general arguments about how these behave in order to get a sense of the general circulation. In the next section we use a specific closure to address the same problem.

Let us summarize the physical situation. The two layers of our model are confined in the vertical direction between two flat, rigid surfaces, and they are meridionally confined between slippery walls at high and low latitudes (the ‘pole’ and ‘equator’). The circulation is driven thermodynamically by heating at low latitudes and cooling at high ones, which translates to a conversion of layer 1 fluid to layer 2 fluid at high latitudes, and the converse at low latitudes (see Fig. 15.12). This sets up an interface that slopes upwards toward the pole and, by thermal wind, a shear. This situation is baroclinically unstable, and this sets up a field of eddies, most vigorous in mid-latitudes where the temperature gradient (or interface slope) is largest. Three fields encapsulate the dynamics — the lower-layer wind field, the meridional circulation, and the meridional temperature gradient, and our goal is to understand their qualitative structure. We note from the outset that the residual circulation is poleward in the upper layer, equatorward in the lower layer, and that this is a thermodynamic result, a consequence of heating at low latitudes and cooling at high latitudes.

From (15.65), the steady-state lower-layer wind is given by

$$rH_2 \overline{u}_2 = H_1 \overline{v'_1 q'_1} + H_2 \overline{v'_2 q'_2} = H_1 \overline{v'_1 \zeta'_1} + H_2 \overline{v'_2 \zeta'_2}, \quad (15.82)$$

where the second equality uses (15.79). That is, *the lower-layer wind is determined by the vertical integral of either the vorticity flux or the potential vorticity flux.*

Neglecting contributions due to the mean horizontal shear (which are small if the *beta-Rossby number*,  $U/\beta L^2$ , is small) the potential vorticity gradient in each layer is given by

$$\frac{\partial \overline{q}_1}{\partial y} = \beta - \frac{f_0}{H_1} \frac{\partial \overline{h}_1}{\partial y} \gg 0 \quad \text{and} \quad \frac{\partial \overline{q}_2}{\partial y} = \beta - \frac{f_0}{H_2} \frac{\partial \overline{h}_2}{\partial y} \leq 0. \quad (15.83a,b)$$

In the upper layer  $\partial \bar{h}_1 / \partial y$  is negative so that the total potential vorticity gradient is positive and larger than  $\beta$  itself. In the lower layer  $\partial \bar{h}_2 / \partial y$  is positive and indeed if there is to be baroclinic instability it must be as large as  $\beta$  in order for  $\partial \bar{q} / \partial y$  to change sign somewhere. Thus, although negative the potential vorticity gradient is much weaker in the lower layer. Thus, Rossby waves (meaning waves that exist because of a background gradient in potential vorticity) will propagate further in the upper layer, and this asymmetry is the key to the production of surface winds.

Now, the potential vorticity flux must be negative (and downgradient) in the upper layer, and there are various ways to see this. One is from the upper-layer momentum equation (15.65a) which in a steady state gives

$$\overline{v'_1 q'_1} = -f_0 \bar{v}_1^*. \quad (15.84)$$

Because  $\bar{v}_1^*$  is poleward,  $f_0 \bar{v}_1^*$  is positive and the potential vorticity flux is negative in both Northern and Southern Hemispheres. Equivalently, in the upper layer the radiative forcing is increasing the potential vorticity gradient between the equator and the pole, so there must be an equatorward potential vorticity flux to compensate. Finally, the perturbation enstrophy or pseudomomentum equations tell us that in a steady state the potential vorticity flux is downgradient (also see Section 15.3.2). This is not an independent argument, since it merely says that the enstrophy budget may be balanced through a balance between production proportional to the potential vorticity gradient and the dissipation. For similar reasons we expect the potential vorticity flux to be positive (poleward) in the lower layer.

Now, (15.80) tells us that the latitudinally integrated potential vorticity flux is equal and opposite in the two layers. If the potential vorticity flux in the lower layer were everywhere equal and opposite to that in the upper layer, then using (15.82) there would be no surface wind, in contrast to the observations. In fact, the potential vorticity flux is more uniformly distributed in the upper layer, and this gives rise to the surface wind observed. Let us give a couple of perspectives (on the same argument) as to why this should be so. The argument centres around the fact that the potential vorticity gradient is stronger in the upper layer, as we can see from (15.83).

### I. Rossby waves and the vorticity flux

The stronger potential vorticity gradient of the upper layer is better able to support linear Rossby waves than the lower layer. Thus, the vorticity flux in the region of Rossby-wave genesis in mid-latitudes will be large and positive in the upper layer, and small and negative in the lower layer. Thus, there will be more momentum convergence into the source region in the upper layer than in the lower layer, and the vertical integral of the vorticity flux will largely be dominated by that of the upper layer. This is positive in mid-latitudes and, to ensure that its latitudinal integral is zero, it is negative on either side. Using (15.82), a surface wind has the same pattern as the net vorticity flux, and so is eastward in the mid-latitude source region and westward on either side.

### II. Potential vorticity flux

Rossby waves are generated in the region of baroclinic instability, at approximately the same latitude in both upper and lower layers. However, because the potential vorticity gradient is larger in the upper layer than in the lower layer, Rossby waves are able to propagate more efficiently and breaking and associated dissipation will tend to be further from the source region in the upper layer than in the lower layer. Now, the pseudomomentum equation for each layer is, similarly to (15.50) for the one-layer case,

$$\frac{\partial \mathcal{P}_i}{\partial t} = \frac{\partial}{\partial t} \left( \frac{\overline{q_i'^2}}{2\gamma_i} \right) = -\overline{v'_i q'_i} - \frac{D'_i q'_i}{\gamma_i}, \quad i = 1, 2, \quad (15.85)$$

where  $\gamma_i$ , the potential vorticity gradient, has opposite signs in each layer. In a statistically steady state, the region of strongest dissipation is the region where the potential vorticity



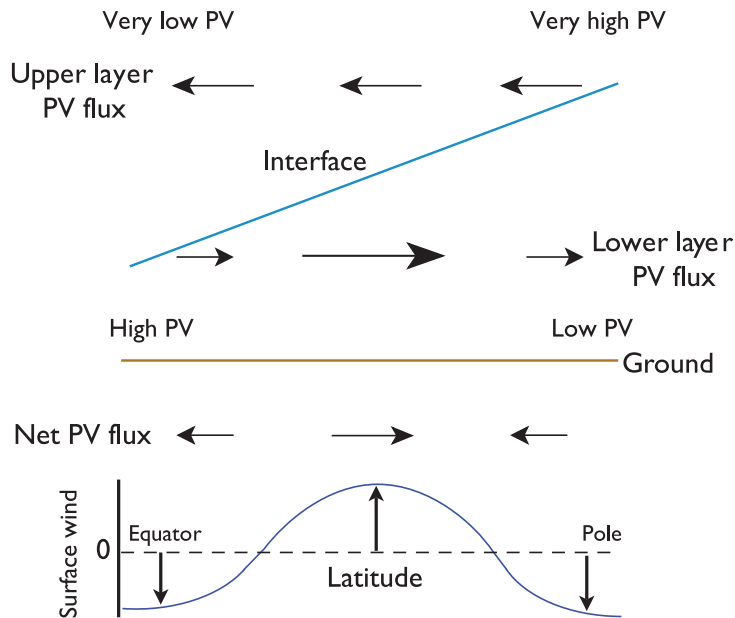


**Fig. 15.13** The upper panel sketches the potential vorticity fluxes in each layer in a two-layer model. The surface wind is proportional to their vertical integral. The PV fluxes are negative (positive) in the upper (lower) layer, but are more uniformly distributed at upper levels.

The lower panel shows the net (vertically integrated) PV fluxes and the associated surface winds. In both panels the  $x$ -axis is latitude.

flux is largest. In the upper layer, Rossby-wave propagation allows the dissipation region to spread out from the source, whereas in the lower layer the dissipation region will be concentrated near the source. The distribution of the potential vorticity flux then becomes as illustrated in Fig. 15.13. The surface winds, being the vertical integral of the potential vorticity fluxes, are westerly in the baroclinic region and easterly to either side.

### Momentum balance and the overturning circulation

From thermodynamic arguments we deduced that the residual circulation is direct, meaning that warm fluid rises at low latitudes, moves poleward aloft, and returns near the surface. At low latitudes where eddy effects are small the zonally-averaged Eulerian circulation circulates in the same way, giving us the Hadley Cell. In mid-latitudes, we may determine the Eulerian circulation from the momentum equation, (15.60). In the upper layer the balance is between the vorticity flux and the Coriolis term, namely

$$f_0 \bar{v}_1 = -\overline{v'_1 \zeta'_1} < 0. \quad (15.86)$$

That is, *the mean Eulerian flow is equatorward*, and this is the upper branch of the Ferrel cell. Note that the Eulerian circulation is in the opposite sense to the residual circulation.

In the lower layer the vorticity fluxes are weak and the balance is largely between the Coriolis force on the meridional wind and the frictional force on the zonal wind (as in Fig. 14.17). If the upper-layer flow is equatorward, the lower-layer flow must be poleward by mass conservation, and so the zonal wind is positive (eastward); that is

$$r \bar{u}_2 \approx f_0 \bar{v}_2 = -\frac{H_1}{H_2} f_0 \bar{v}_1 > 0, \quad (15.87a,b)$$

where the second equality follows by mass conservation of the Eulerian flow.

In terms of the TEM form of the equations, (15.65), the corresponding balances in the centre of the domain are

$$f_0 \bar{v}_1^* = -\overline{v'_1 q'_1} > 0 \quad (15.88a)$$

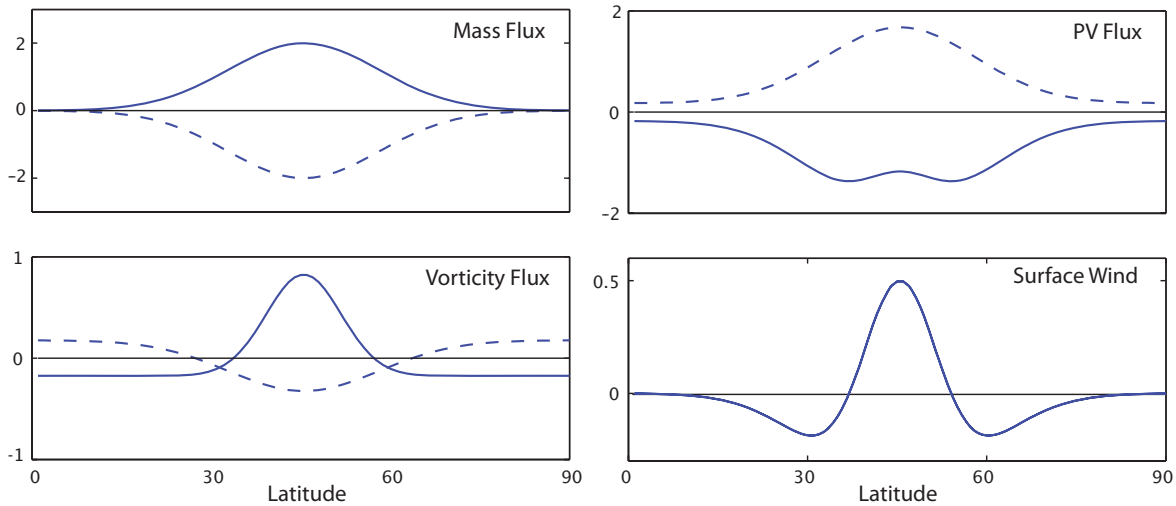


**Fig. 15.14** Eddy fluxes in a two-layer model of an atmosphere with a single mid-latitude baroclinic zone. The upper-layer fluxes are solid lines and the lower-layer fluxes are dashed. The bottom-right panel shows the sum of the lower- and upper-layer vorticity fluxes (or, equivalently, the sum of the potential vorticity fluxes), which is proportional (when the surface friction is a linear drag) to the surface wind. The fluxes satisfy the various relationships and integral constraints of Section 15.2.2 but are otherwise idealized.

and

$$r\bar{u}_2 = f_0\bar{v}_2^* + \overline{v_2'q_2'} = -f_0\frac{H_1}{H_2}\bar{v}_1^* + \overline{v_2'q_2'} = \frac{H_1}{H_2}\overline{v_1'q_1'} + \overline{v_2'q_2'} > 0, \quad (15.88b)$$

using mass conservation and the fact that the lower-layer potential vorticity fluxes are larger than those of the upper layer. Illustrations of the dynamical balances of the two-layer model are given in Figs. 15.13 and 15.14.

### 15.3 † EDDY FLUXES AND AN EXAMPLE OF A CLOSED MODEL

The arguments above are heuristic and phenomenological and, although quite plausible, they are not wholly systematic. In this section we give a more axiomatic calculation by making certain closure assumptions that relate the eddy fluxes to the mean fields; specifically, we invoke the diffusion of potential vorticity, and then calculate the zonal winds and meridional circulation. The main purpose of this section is to explicitly show that if we do invoke a potential vorticity closure then a complete solution of the flow follows. However, too much credence should not be given to the particular closure we do invoke, for it cannot be rigorously justified.

#### 15.3.1 Equations for a Closed Model

With quasi-geostrophic scaling, the equations of motion are the momentum equations written in residual form,

$$\frac{\partial \bar{u}_1}{\partial t} = f_0\bar{v}_1^* + \overline{v_1'q_1'}, \quad (15.89a)$$

$$\frac{\partial \bar{u}_2}{\partial t} = f_0\bar{v}_2^* + \overline{v_2'q_2'} - r\bar{u}_2, \quad (15.89b)$$

and the mass conservation equation for each layer which may be written as an equation for the interface height,

$$\frac{\partial \bar{\eta}}{\partial t} - H_1 \frac{\partial \bar{v}_1^*}{\partial y} = S, \quad (15.90)$$

where  $\eta = H_1 - h_1 = h_2 - H_2$ , with the notation of the previous sections. This can be written in terms of  $\bar{v}_2^*$  because

$$H_1 \bar{v}_1^* + H_2 \bar{v}_2^* = 0. \quad (15.91)$$

The velocities and thickness of the layers are related by the thermal wind relation

$$f_0(\bar{u}_1 - \bar{u}_2) = g' \frac{\partial \bar{\eta}}{\partial y} = -g' \frac{\partial \bar{h}_1}{\partial y}. \quad (15.92)$$

Using this to eliminate time derivatives between (15.89) and (15.90) reveals that the residual circulation satisfies

$$f_0^2 \frac{H}{H_2} \bar{v}_1^* - H_1 g' \frac{\partial^2 \bar{v}_1^*}{\partial y^2} = +g' \frac{\partial S}{\partial y} - f_0 (\overline{v_1' q_1'} - \overline{v_2' q_2'}) - f_0 r \bar{u}_2, \quad (15.93)$$

where  $H = H_1 + H_2$ . Thus, *the residual circulation is driven by the potential vorticity fluxes*, plus the diabatic terms. We may derive a similar expression for the Eulerian mean meridional flow, namely

$$f_0^2 \frac{H}{H_2} \bar{v}_1 - H_1 g' \frac{\partial^2 \bar{v}_1}{\partial y^2} = g' \frac{\partial S}{\partial y} + g' \frac{\partial^2}{\partial y^2} \overline{v_1' h_1'} - f_0 (\overline{v_1' \zeta_1'} - \overline{v_2' \zeta_2'}) - f_0 r \bar{u}_2. \quad (15.94)$$

However, the right-hand side now involves *both* the eddy vorticity fluxes and the eddy mass fluxes. The above equations illustrate the natural way in which the potential vorticity fluxes proximately 'drive' the extratropical atmosphere (see also the box on page 566).

### Potential vorticity equation

A single prognostic equation for each layer is obtained by eliminating the residual circulation from (15.89) and (15.90), giving

$$\frac{\partial \bar{q}_1}{\partial t} = -\frac{\partial \overline{v_1' q_1'}}{\partial y} + \frac{f_0}{H_1} S, \quad (15.95a)$$

$$\frac{\partial \bar{q}_2}{\partial t} = -\frac{\partial \overline{v_2' q_2'}}{\partial y} - \frac{f_0}{H_2} S + r \frac{\partial \bar{u}_2}{\partial y}, \quad (15.95b)$$

where  $q_i$  are the quasi-geostrophic potential vorticities of each layer given by

$$\bar{q}_1 = -\frac{\partial \bar{u}_1}{\partial y} + f_0 \frac{\bar{\eta}}{H_1}, \quad \bar{q}_2 = -\frac{\partial \bar{u}_2}{\partial y} - f_0 \frac{\bar{\eta}}{H_2}. \quad (15.96a,b)$$

### Closure

If the potential vorticity fluxes can be expressed in terms of the mean fields then (15.95) is a closed set of equations. We can then solve for the potential vorticity in each layer and, using (15.93), for the residual circulation. One simple and rational closure is to assume that potential vorticity flux is transferred downgradient so that

$$\overline{v_i' q_i'} = -K_i \frac{\partial \bar{q}_i}{\partial y}, \quad (15.97)$$

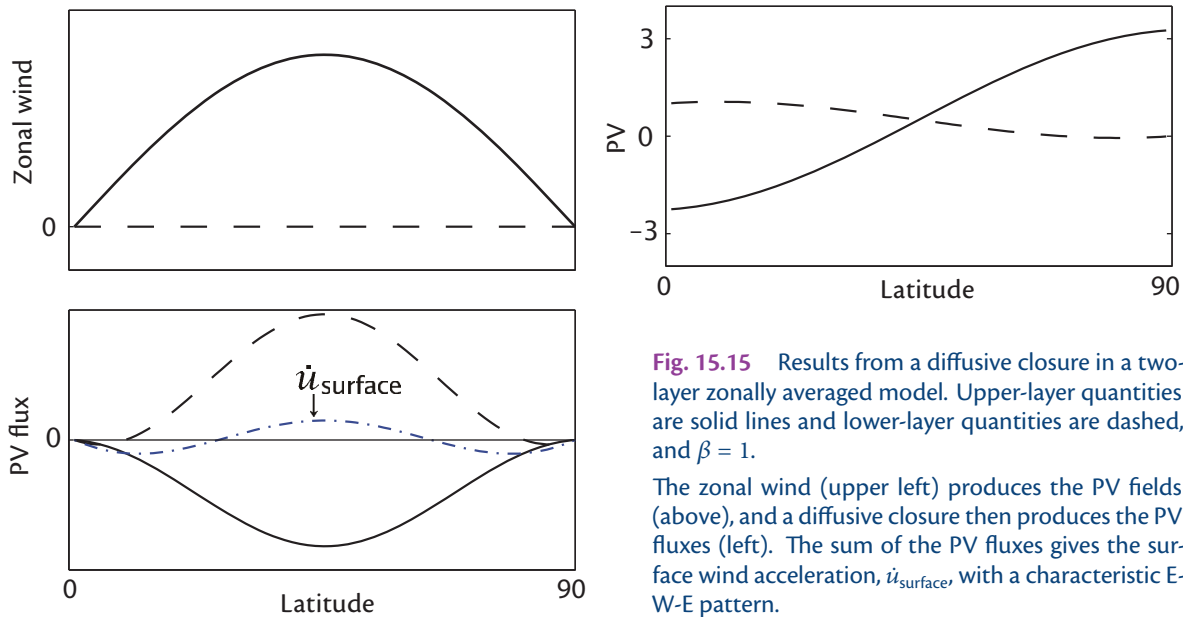


**Fig. 15.15** Results from a diffusive closure in a two-layer zonally averaged model. Upper-layer quantities are solid lines and lower-layer quantities are dashed, and  $\beta = 1$ .

The zonal wind (upper left) produces the PV fields (above), and a diffusive closure then produces the PV fluxes (left). The sum of the PV fluxes gives the surface wind acceleration,  $\ddot{u}_{\text{surface}}$ , with a characteristic E-W-E pattern.

where  $K_i$  is an eddy diffusivity, or transfer coefficient, which here is just a scalar quantity.<sup>5</sup> Note that the model demands a closure of the potential vorticity flux — not momentum, vorticity or the mass flux — and potential vorticity, being a materially conserved variable, is also that field for which a diffusive closure is most applicable.

Such a closure has all of the features and problems associated with diffusive closures discussed in Chapter 13, plus some of its own. One is that such a diffusive closure will not automatically respect the kinematic constraint that the volume integral of the potential vorticity flux must vanish, which for the two-layer model is expressed by (15.80). We may *choose* the vertical structure of the diffusivity in such a way that this constraint is satisfied, and in that case the model produces the results illustrated in Fig. 15.15.

The diffusive closure does indeed then produce potential vorticity fluxes similar to the observed westward–eastward–westward surface wind pattern, and a residual circulation of the same sense as in Fig. 15.12, and constitutes perhaps the simplest closed model of the zonally-averaged atmospheric circulation. Note that the surface wind is produced by the integral of the potential vorticity flux and, because the fluxes are quite different in the two layers, two layers are needed to produce a realistic pattern of surface wind without oversimplification, as well as to represent the meridional overturning and residual circulations. However, the model is a little ad hoc and the results depend on the structure of the transfer coefficients and the boundary conditions chosen.

### 15.3.2 ♦ Necessary Conditions for a Statistically Steady State

In linear baroclinic instability problems, a necessary condition for instability (the Charney–Stern–Pedlosky, or CSP, condition) is that the potential vorticity change sign in the interior of the fluid, or that the potential vorticity gradient in the interior has a particular sign with respect to the buoyancy gradient at horizontal bounding surfaces, as discussed in Chapters 9 and 10. These conditions do not apply in the statistical steady state of the forced-dissipative problem, but we may derive related conditions that do, although they are not completely general. We will focus on the interior condition and not the boundary conditions, as is appropriate in a layered model, but the argument could be extended to cover boundary issues explicitly.

The linear perturbation potential vorticity equation is

$$\frac{\partial q'}{\partial t} = -\bar{u} \frac{\partial q'}{\partial x} - v' \frac{\partial \bar{q}}{\partial y} - D', \quad (15.98)$$

where  $D'$  represents dissipative processes. From this we form the enstrophy equation

$$\frac{1}{2} \frac{\partial \overline{q'^2}}{\partial t} + \overline{D'q'} = -\overline{v'q'} \frac{\partial \bar{q}}{\partial y}, \quad (15.99)$$

where an overbar is a zonal average and we generally assume  $\overline{D'q'} > 0$ , as with a linear drag on  $q$ . In the standard linear problem we take  $D = 0$  and then for growing waves ( $\partial_t \overline{q'^2} > 0$ ) the right-hand side must be positive. But the integral of  $\overline{v'q'}$  over latitude and height is zero, and thus  $\overline{v'q'}$  must take both positive and negative signs. Hence, for growing waves,  $\partial \bar{q} / \partial y$  must also take both positive and negative signs, and we recover the CSP condition that  $\partial \bar{q} / \partial y$  must change sign for an instability. (We need not assume that the instabilities have normal form. A very similar argument was given in Section 10.6.)

In a statistically steady state the production of variance by the terms on the right-hand side is balanced by a cascade of variance to small scales. The quantity  $\overline{v'q'}$  is non-zero, but its spatial integral still vanishes. We therefore have

$$\int \frac{\overline{D'q'}}{\partial \bar{q} / \partial y} dy dz = - \int \overline{v'q'} dy dz = 0. \quad (15.100)$$

Now,  $\overline{D'q'} > 0$ , and therefore to satisfy the equation  $\partial \bar{q} / \partial y$  must change sign somewhere. That is, in a statistically steady state with dissipation,  $\partial \bar{q} / \partial y$  must be both positive and negative somewhere in the domain. This is an analogue of the CSP result for wave-mean-flow interaction. Furthermore, if (as we have assumed) the left-hand side of (15.99) is positive everywhere, then eddy flux must be downgradient everywhere.

We can go a little further and obtain a result with the nonlinear terms. The zonally-averaged perturbation enstrophy equation is then

$$\frac{1}{2} \frac{\partial \overline{q'^2}}{\partial t} = -\overline{v'q'} \frac{\partial \bar{q}}{\partial y} - \frac{1}{2} \frac{\partial}{\partial y} \overline{v'q'^2} - \overline{D'q'}. \quad (15.101)$$

On integrating in  $y$  the third-order term vanishes and we obtain

$$\int \left( \frac{1}{2} \frac{\partial}{\partial t} \overline{q'^2} + \overline{D'q'} \right) dy = - \int \overline{v'q'} \frac{\partial \bar{q}}{\partial y} dy, \quad (15.102)$$

and so, if the left-hand side is positive, the flux must still be downgradient in the integrated sense that

$$\int \overline{v'q'} \frac{\partial \bar{q}}{\partial y} dy < 0. \quad (15.103)$$

Suppose that the flux is *locally* downgradient, meaning that  $\partial \bar{q} / \partial y$  and  $\overline{v'q'}$  have opposite signs, and in the nonlinear case this is an additional physical assumption. Then, because  $\overline{v'q'}$  has both positive and negative values (because its integral is zero), then so must the potential vorticity gradient,  $\partial \bar{q} / \partial y$ . That is, *when dissipation is present and if the potential vorticity fluxes are downgradient, a statistically steady state can be maintained only if the potential vorticity gradient changes sign somewhere*. In the continuously stratified case, this condition is replaced by ones involving a combination of the interior potential vorticity gradient and the buoyancy gradient at the boundary, the conditions being the same as necessary conditions for instability.

### Potential Vorticity Fluxes and the Extratropical Atmosphere

The extratropical circulation of the atmosphere is driven by the differential heating between equator and pole, mediated by fluxes of potential vorticity. Thus, in a layered model we have the following:

- (i) *Zonal winds.* At each level the acceleration of the zonal winds is governed by the potential vorticity fluxes:

$$\frac{\partial \bar{u}_i}{\partial t} = \bar{v}_i' \bar{q}_i' + f_0 \bar{v}_i^* + F_i, \quad (\text{PV.1})$$

where  $\bar{v}_i^*$  is the residual meridional flow and  $F_i$  represents friction.

- (ii) *Surface winds.* In steady state, the surface winds are produced by the vertically integrated potential vorticity fluxes:

$$r H_s \bar{u}_s = \sum_i H_i \bar{v}_i' \bar{q}_i', \quad (\text{PV.2})$$

where  $u_s$  is the surface wind,  $H_s$  the thickness of the lowest layer, and  $r$  is a frictional coefficient.

- (iii) *Meridional transport.* The total (or residual) meridional transport is, proximately, forced by the potential vorticity fluxes. For example, in a two-layer model

$$f_0^2 \frac{H}{H_2} \bar{v}_1^* - H_1 g' \frac{\partial^2 \bar{v}_1^*}{\partial y^2} = +g' \frac{\partial S}{\partial y} - f_0 (\bar{v}_1' \bar{q}_1' - \bar{v}_2' \bar{q}_2') - f_0 (F_1 - F_2), \quad (\text{PV.3})$$

where  $S$  is proportional to the diabatic forcing, and this equation holds at all times. In a steady state the momentum equation gives simply

$$f_0 \bar{v}_i^* = -\bar{v}_i' \bar{q}_i' - F_i. \quad (\text{PV.4})$$

Above the surface layer friction is negligible and the meridional transport responds almost solely to the potential vorticity fluxes.

## 15.4 A STRATIFIED MODEL AND THE REAL ATMOSPHERE

In the previous section we introduced the effects of stratification by way of a two-layer model. Let us now discuss, albeit rather qualitatively, the dynamics of a continuously stratified model more relevant to the real atmosphere. These dynamics are generally similar to that of the two-layer model, although a number of differences in interpretation do arise. In particular, rather than the potential vorticity flux in the two layers, it is the potential vorticity flux in the interior and the buoyancy flux near the boundary that are the key aspects in producing the mean circulation.

### 15.4.1 Potential Vorticity and its Fluxes

The observed zonally-averaged potential vorticity field is shown in Fig. 15.16. Of interest to us is the fact that over most of the atmosphere, over most of the year, the potential vorticity gradient is monotonic, with the potential vorticity increasing northward. (The potential vorticity in the troposphere also increases moving northward along isentropes.) How, then, can the atmosphere be baroclinically unstable? It is because the surface buoyancy (or temperature) decreases poleward,

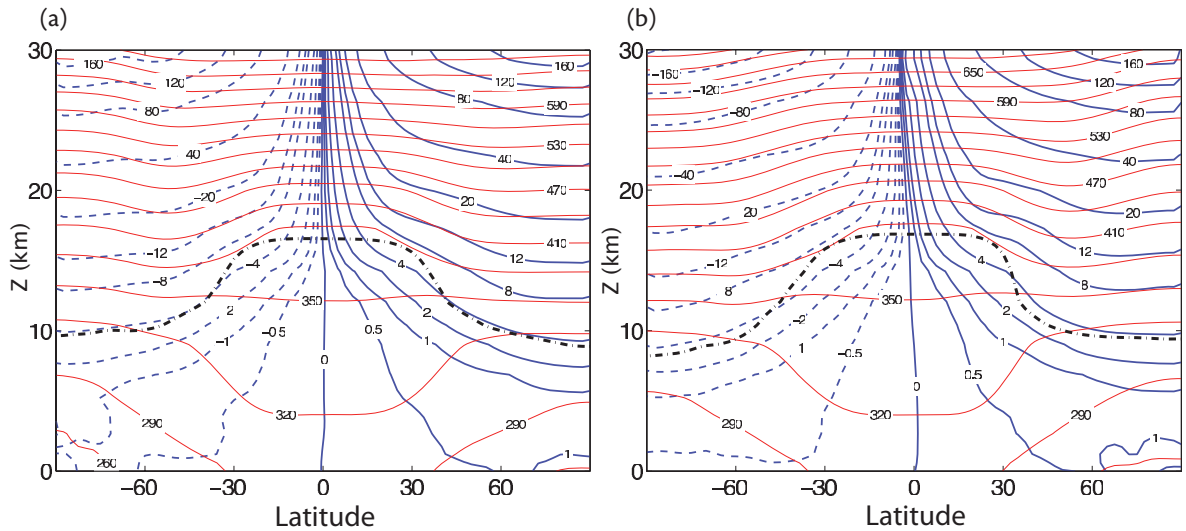


**Fig. 15.16** The observed zonally-averaged Ertel potential vorticity distribution (dark solid and dashed lines, peaking up at the equator) and the potential temperature (lighter, red lines) for (a) annual mean, (b) December–January–February. Also shown is the position of the thermal tropopause (black, dot-dashed line). The potential vorticity is in ‘PV units’,  $1 \text{ PVU} \equiv 1.0 \times 10^{-6} \text{ m}^2 \text{ K s}^{-1} \text{ kg}^{-1}$ , and has uneven contour intervals. The vertical coordinate is log pressure, with  $Z = -H \log(p/p_R) \text{ km}$ , where  $p_R = 10^5 \text{ Pa}$  and  $H = 7.5 \text{ km}$ .

and thus the atmosphere becomes unstable via the interaction of a surface edge wave with an interior Rossby wave (see the conditions on page 351 or page 404). This baroclinic instability may then excite Rossby waves which propagate meridionally, producing a momentum convergence and westward surface flow, and an associated meridional circulation or Ferrel Cell, much as described in Section 15.1. Let us explore these phenomena in a little more detail.

### Surface winds

Consider the zonally-averaged, continuously stratified momentum equations with quasi-geostrophic scaling,

$$\frac{\partial \bar{u}}{\partial t} = \overline{v' \zeta'} + f_0 \bar{v} + F = \overline{v' q'} + f_0 \bar{v}^* + F, \quad (15.104)$$

where  $F$  represents frictional effects and the residual velocity  $\bar{v}^*$  is given by

$$\bar{v}^* = -\frac{\partial \psi^*}{\partial z} = \bar{v} - \frac{\partial}{\partial z} \left( \frac{1}{N^2} \overline{v' b'} \right). \quad (15.105)$$

The friction is given by the vertical gradient of a stress,  $F = \partial \tau / \partial z$ , and at the surface we may parameterize the stress, following (5.210) on page 208, by  $\tau = r \bar{u}$  where  $r$  is a constant. Then, vertically integrating (15.104) from the surface to the top of the atmosphere (where frictional stresses and the buoyancy flux both vanish) we find, in steady state,

$$r \bar{u}(0) = \langle \overline{v' \zeta'} \rangle = \langle \overline{v' q'} \rangle + \frac{f_0}{N^2} \overline{v' b'}(0), \quad (15.106)$$

where the angle brackets denote a vertical integral and (0) denotes surface values. Thus, the surface winds are determined, analogously to (15.82), by the vertically integrated relative vorticity fluxes, or equivalently by the integral of the interior potential vorticity fluxes and the buoyancy fluxes at



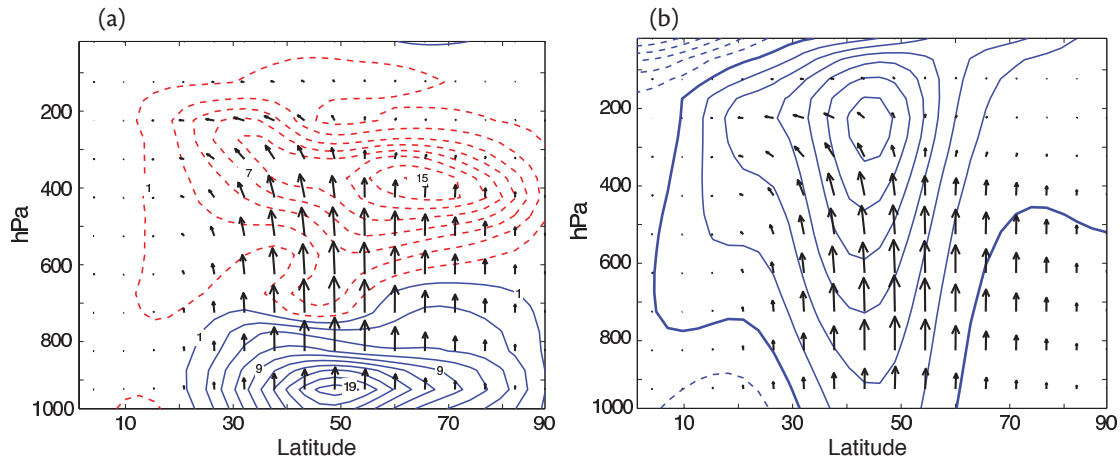


**Fig. 15.17** The Eliassen–Palm flux in an idealized primitive equation of the atmosphere. (a) The EP flux (arrows) and its divergence (contours, with intervals of  $2 \text{ m s}^{-1}/\text{day}$ ). The solid contours denote flux divergence, a positive PV flux, and eastward flow acceleration; the dashed contours denote flux convergence and deceleration. (b) The EP flux (arrows) and the time and zonally-averaged zonal wind (contours). See the Appendix A for details of plotting EP fluxes.

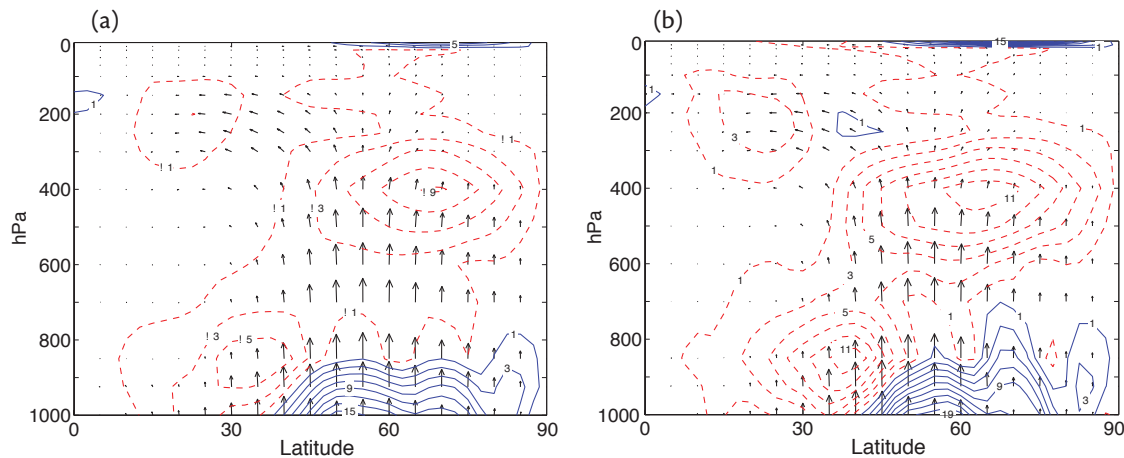


**Fig. 15.18** The observed Eliassen–Palm flux (arrows) and its divergence (contours, with intervals of  $2 \text{ m s}^{-1}/\text{day}$ , zero contour omitted) in the Northern Hemisphere. Solid contours denote divergence, a positive (eastward) torque on the flow, and dashed contours denote convergence, a westward torque. (a) Annual mean, (b) DJF (December–January–February).

the surface. The advantage of the latter representation is that both potential vorticity and buoyancy are materially conserved variables and it may be easier to deduce some properties of their fluxes than of the fluxes of relative vorticity. Compared to the two-layer formulation, the interior fluxes are analogous to those of the upper layer whereas the surface fluxes are analogous to those of the lower layer, especially as the lower layer becomes thin.

#### Potential vorticity and Eliassen–Palm fluxes

As in Section 10.2, the quasi-geostrophic potential vorticity flux may be written as the divergence of the Eliassen–Palm (EP) vector,

$$\overline{v'q'} = \nabla_x \cdot \mathcal{F}, \quad (15.107)$$

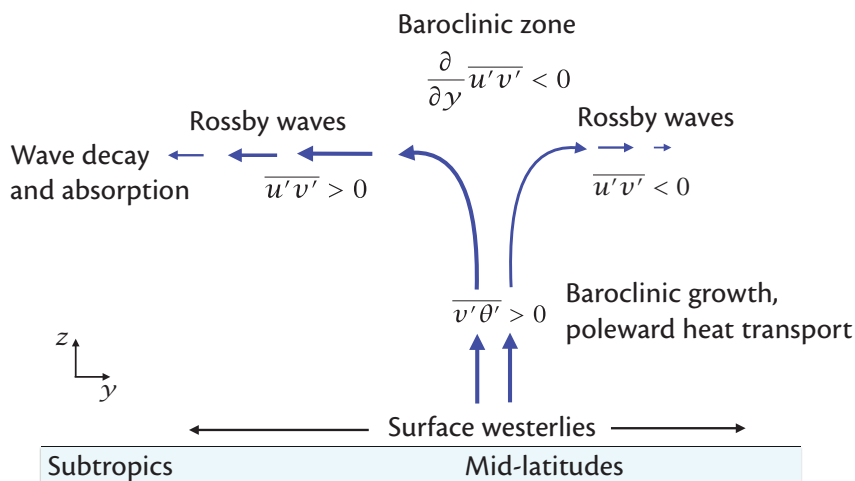


**Fig. 15.19** Schematic of Eliassen-Palm fluxes in a baroclinic atmosphere. The vertical component,  $\overline{v'\theta'}$  (or  $\overline{v'b'}$ ) occurs primarily during the growing phase of the baroclinic lifecycle and corresponds to a poleward heat flux. The meridional fluxes in the upper atmosphere are associated with Rossby waves, and the vertical integral of the momentum flux divergence gives rise to surface westerlies.

where  $\nabla_x \cdot \equiv \mathbf{j} \partial / \partial y + \mathbf{k} \partial / \partial z$  and

$$\mathcal{F} \equiv -\overline{u'v'} \mathbf{j} + \frac{f_0}{N^2} \overline{v'\theta'} \mathbf{k}. \quad (15.108)$$

(See Appendix A to this chapter for primitive equation and spherical coordinate versions; in practice the quasi-geostrophic expression qualitatively captures the dominant terms in the primitive equation expressions.) The EP vector as obtained from an idealized primitive equation general circulation model integration is shown in Fig. 15.17, and the EP vector from observations is shown in Fig. 15.18, and both show qualitatively similar properties — a generally upwards-pointing vector in mid-latitude, veering equatorward aloft (and sometimes with some poleward propagation) as illustrated in Fig. 15.19.

The upward component represents the meridional transfer of heat, and this occurs during the growth phase of the baroclinic lifecycle and is qualitatively captured by linear models — for example, in the Eady problem the EP flux is directed purely vertically (Fig. 10.2), and this aspect resembles the vertical components of Figs. 15.17 and 15.18. But why should the average over a complete baroclinic lifecycle (which Fig. 15.19 schematically represents) even approximately resemble that of the growing phase of the baroclinic lifecycle? After all, the eddies must subsequently decay, and one might imagine that the fluxes would then reverse themselves. In fact, this is not the case: the baroclinic lifecycle is not reversible, because of two effects. First, there is transfer of baroclinic energy to barotropic modes (as described in Chapter 12) followed by a barotropic decay. Thus, over the complete cycle, there is no downwelling branch of EP fluxes that would correspond to equatorward heat transfer, and on average the poleward heat transfer (the  $\overline{v'\theta'}$  branch) balances the net atmospheric heating. Second, there is an irreversible absorption and decay of the Rossby waves emanating from the baroclinic zone. These Rossby waves give rise to the lateral component of the EP flux, much as described in Section 15.1, although the wave activity is predominantly in the upper troposphere where the potential vorticity gradient is larger. This propagation is an irreversible process since the Rossby waves break and dissipate some distance from their source; this dissipation breaks the non-acceleration conditions and provides the mean flow acceleration and, consequentially, the observed zonal wind

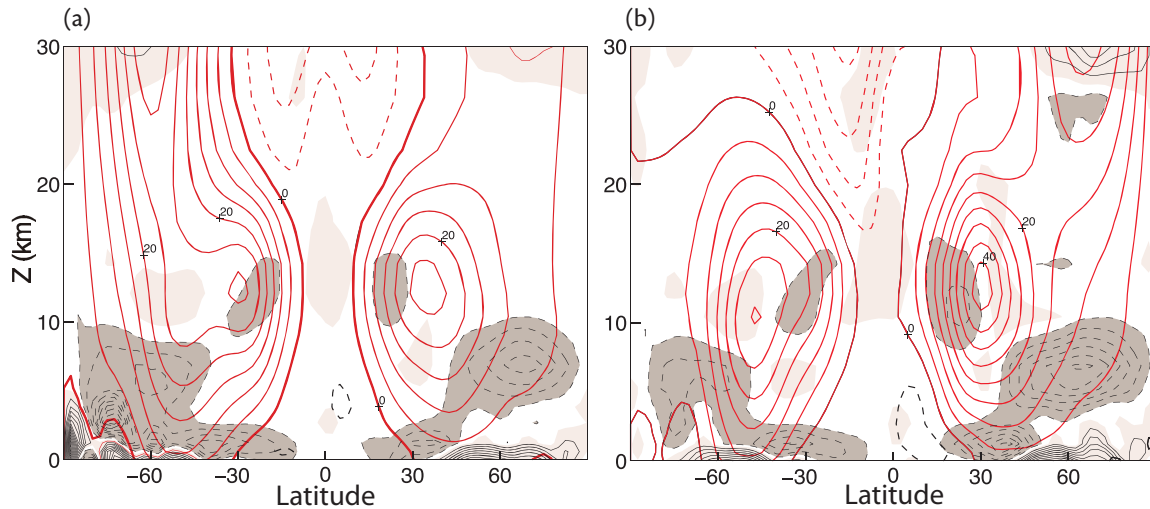


**Fig. 15.20** The observed zonally-averaged zonal wind (thicker, red, contours, interval  $5 \text{ m s}^{-1}$ ), and the Eliassen–Palm flux divergence (contour interval  $2 \text{ m s}^{-1}/\text{day}$ , zero contour omitted). Regions of positive EP flux divergence (eastward acceleration) are lightly shaded; regions less than  $-2 \text{ m s}^{-1}/\text{day}$  are more darkly shaded. (a) Annual mean, (b) DJF (December–January–February).

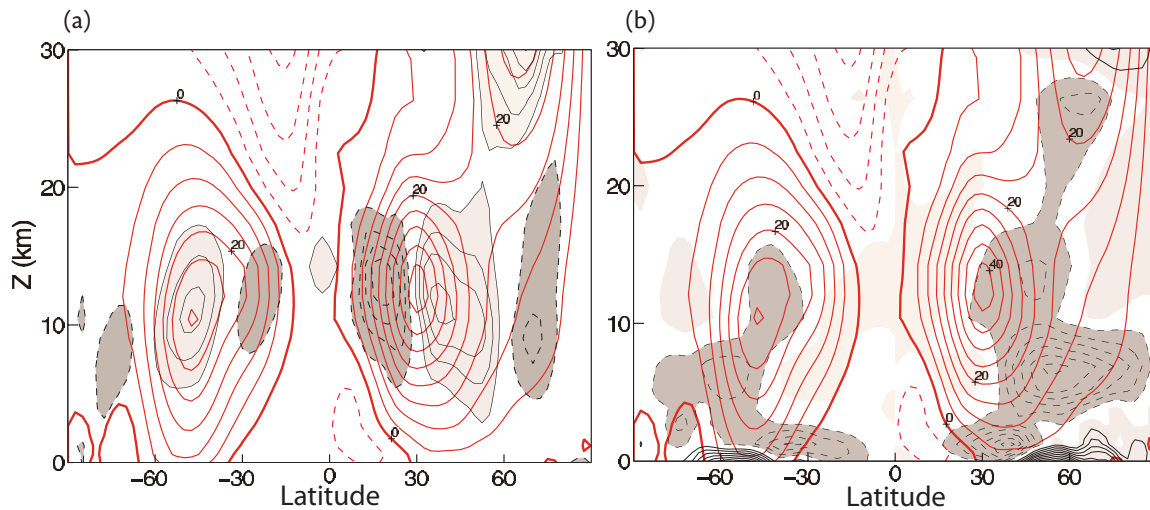


**Fig. 15.21** The divergence of the two components of the EP flux (shaded), and the zonally-averaged zonal wind (thicker, red, contours) for DJF. (a) The momentum fluxes,  $-\partial_z \overline{u'v'}$ , contour interval is  $1 \text{ m s}^{-1}/\text{day}^{-1}$ , light shaded for positive values  $> 1$ , dark shaded for negative values  $< -1$ . (b) The buoyancy flux,  $f \partial_z (\overline{v'b'}) / N^2$ , with contour interval and shading convention as in Fig. 15.20.

The divergence of the EP flux — that is, the potential vorticity flux — accelerates (or decelerates) the mean flow, as can be seen from (15.104) and Fig. 15.20. Broadly speaking, the EP flux decelerates the flow aloft (where it is balanced by the Coriolis force on the poleward residual flow) but provides an eastward acceleration at the surface (where it is largely balanced by friction). However, the two components of the flux (Fig. 15.21) have rather different effects on the mean flow. The horizontal component acts to extract momentum from the subtropics and deposit it in mid-latitudes, and so accelerate the flow producing a fairly barotropic eastward jet. (It is this component

that gives rise to so-called negative viscosity, in which the eddies transfer momentum upgradient.) The vertical component of the EP flux arises from the meridional buoyancy flux and acts to reduce the intensity of the mid-latitude westerlies aloft, transferring momentum to the surface where it may be balanced by friction, and producing the surface westerlies. Two questions spring to mind:

- (i) Why is the meridional wave-activity propagation predominantly in the upper atmosphere? That is to say, why do the EP vectors only veer laterally above about 400 hPa, and not in the lower atmosphere?
- (ii) Why is the wave-activity propagation (the direction of the EP flux vectors) predominantly equatorward?

As regards item (i), the propagation is mainly in the upper atmosphere because it is here that the potential vorticity gradient is strongest, as can be seen from Fig. 15.16. In the upper troposphere the beta effect is reinforced by the thermodynamic vortex stretching term, whereas the two effects partial cancel in the lower troposphere, an effect that is seen most clearly in a two-layer model (for example, Fig. 15.15). Thus, wave propagation is more efficient in the upper troposphere, whereas the lower troposphere is more nonlinear and so here the enstrophy cascade, and wavebreaking, occur locally and closer to the region of baroclinic instability itself. Regarding item (ii), the proximate reason is that waves predominantly break on the equatorial side of the instability, and this in turn is for two possible reasons. One is that  $\beta$  increases towards the equator, so that linear propagation is more dominant. The other is that there is often a critical layer in the subtropics, where the speed of the waves equals that of the flow itself ( $\bar{u} = c$ ), and here breaking can efficiently occur.

### 15.4.2 Overturning Circulation

The Eulerian overturning circulation (meaning the circulation from a conventional zonal average at constant height) in mid-latitudes is a single indirect cell, the Ferrel Cell, with rising motion at high latitudes and sinking in the subtropics (top panel of Fig. 15.22). The residual circulation is direct and, consistent with the theory of Section 10.3.3, resembles closely the thickness-weighted circulation. The observed circulation is shown in Fig. 15.22 with a schematic in Fig. 15.23. The main features are qualitatively captured by the two-layer dynamics of Section 15.2.2, but the continuously stratified case differs in some respects.

The main difference between the continuous and two-layer cases is that in the former the return flows — both the lower branch of the Ferrel Cell and the equatorial branch of the residual circulation — are not distributed over the lower troposphere, but are confined to a relatively thin layer. In the lower branch of the Ferrel Cell the dynamical balance is between friction and the Coriolis force on the meridional flow, so that its thickness is that of a turbulent Ekman layer and about a kilometre. To understand this better, let us take a quasi-geostrophic perspective. The mean potential vorticity gradient in the free atmosphere is nearly everywhere poleward and the potential vorticity flux is largely downgradient and equatorward. This means that here the residual circulation is largely poleward, satisfying the balance

$$f\bar{v}^* \approx -\overline{v'q'}. \quad (15.109)$$

In a multi-layer quasi-geostrophic model, with friction acting only in the lowest layer, the circulation is closed by return flow in the lowest layer; thus, as the number of layers increases the return flow is carried in an ever-thinner layer, this becoming a delta-function in the continuous limit, just as in the example of residual flow in the Eady problem (Section 10.5). In the real atmosphere, the return flow cannot be confined to a delta-function, but this argument suggests that it will occur close to the surface and this expectation is borne out in the lower panels of Fig. 15.22 and in Fig. 14.16. In fact, much of the equatorial return flow occurs in isentropic layers that have a potential temperature below the mean value at the surface — that is, in cold air outbreaks.

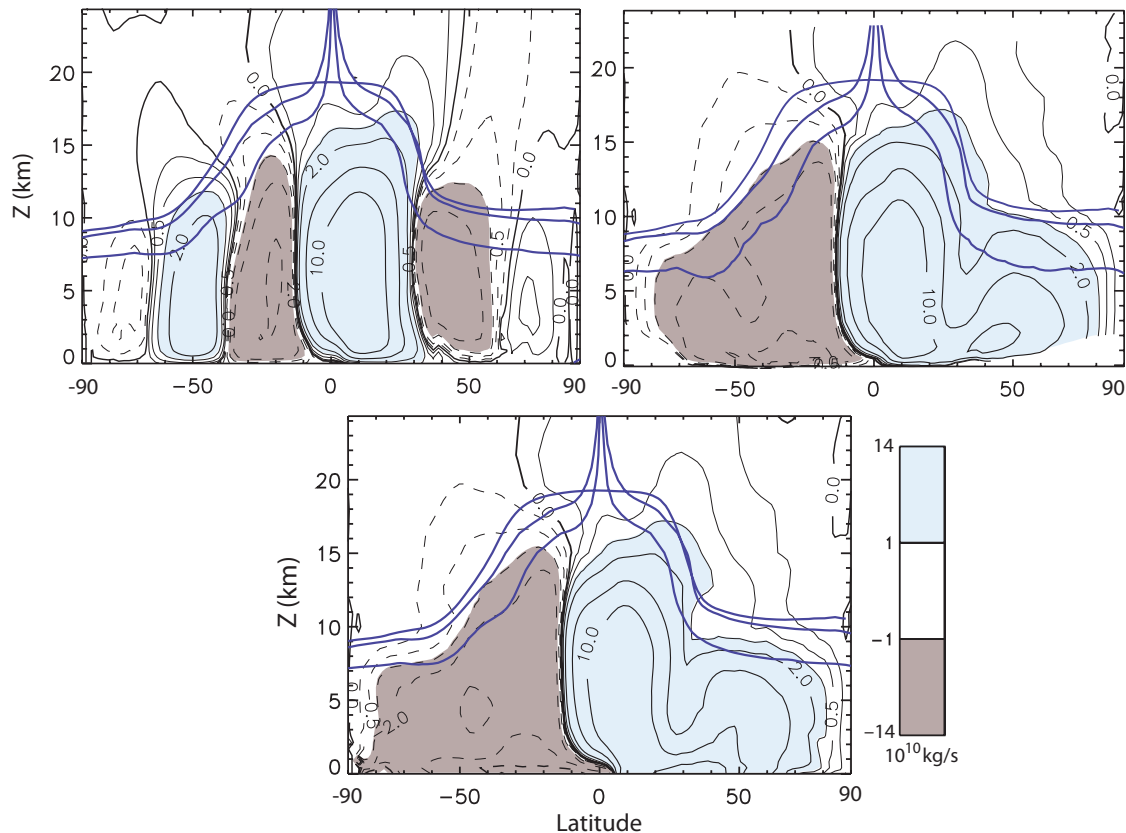


**Fig. 15.22** Top left: The observed zonally-averaged, Eulerian-mean, streamfunction in Northern Hemisphere winter (DJF, 1994–1997). Negative contours are dashed, and values greater or less than  $10^{10} \text{ kg s}^{-1}$  ( $10 \text{ Sv}$ ) are shaded, darker for negative values. The circulation is clockwise around the lighter shading. The three thick solid lines indicate various measures of the tropopause: the two that peak at the equator are isolines of potential vorticity,  $Q = \pm 1.5, \pm 4 \text{ PV units}$ , and the flatter one is the thermal tropopause. Top right: The thickness-weighted meridional mass streamfunction. After calculation in isentropic coordinates, the streamfunction is projected back on to log-pressure coordinates for display. Bottom: the residual streamfunction calculated from the Eulerian circulation and the eddy fluxes.<sup>6</sup>

### 15.5 † TROPOPAUSE HEIGHT AND THE STRATIFICATION OF THE TROPOSPHERE

Let us now explore the physical processes that determine atmospheric stratification. The atmosphere may be divided by stratification into certain distinct regions, illustrated in Fig. 15.24 and Fig. 15.25. The left panel of Fig. 15.24 shows the so-called ‘US standard atmosphere’, a rough average temperature profile and a sometimes-useful standard, as well as actual observed values in the lower atmosphere. In the lower 10 km or so of the atmosphere we have the *troposphere*, a dynamically active region wherein most of the weather and the vast predominance of heat transport occurs. The troposphere is capped by the *tropopause*, above which lies the *stratosphere*, a region of stable stratification extending upwards to about 50 km. (Troposphere means ‘turning sphere’, appropriately so as within it dynamical overturning is prevalent. Stratosphere means ‘layered sphere’, and here there is much less vertical motion.) The stratosphere is capped by the *stratopause*, above which are the mesosphere, thermosphere and exosphere, regions of the upper atmosphere that do not concern us here. Our focus will be on the processes that determine the stratification of the lower atmosphere and the height of the tropopause.<sup>7</sup>

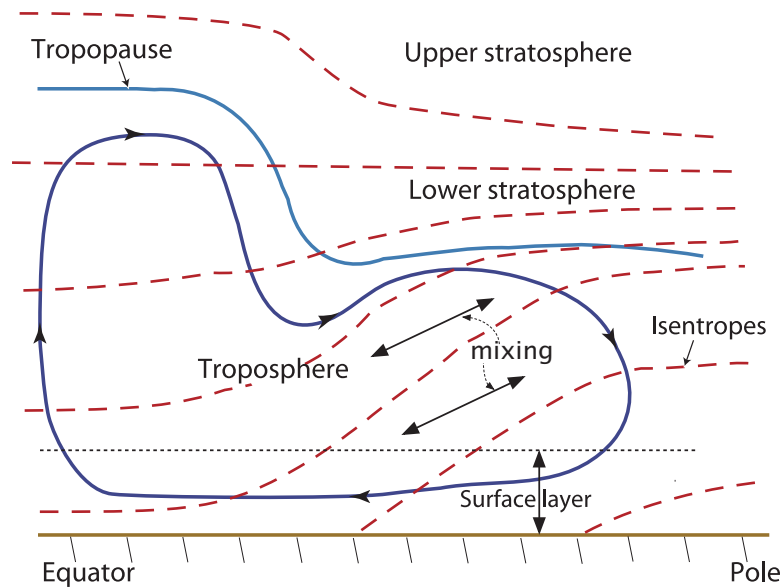


**Fig. 15.23** Schematic of the stratification and residual overturning circulation in the lower atmosphere. The overturning circulation has two distinct parts, a tropical Hadley Cell where the large-scale flow is largely zonally-symmetric and a shallower extratropical cell where the heat and momentum transfer occurs in eddying motion. The equatorward return flow is mostly confined to a shallow surface layer. The lower stratosphere is ventilated by the troposphere along isentropic surfaces, whereas in the upper stratosphere isentropes do not intersect the tropopause. The tropopause is the boundary between the partially mixed troposphere and the near-radiative equilibrium stratosphere. Mixing tends to occur along slopes somewhat shallower than the isentropes.

In the troposphere temperature generally falls with height, whereas in the stratosphere it increases with height, and this gives rise to a thermal definition of the tropopause:<sup>8</sup> *The tropopause is the lowest level at which the lapse rate decreases to  $2 \text{ K km}^{-1}$  or less, provided also that the average lapse rate between this level and all higher levels within 2 km does not exceed  $2 \text{ K km}^{-1}$ .* At any particular time there might also be a second tropopause: if above the first tropopause the average lapse rate between any level and all higher levels within 1 km exceed  $3 \text{ K km}^{-1}$ , then a second (higher) tropopause is defined by that same criterion. Finally, such definitions are presumed not to apply if they are satisfied below 500 mb. As so defined, the thermal tropopause typically varies in height from about 16 km at low latitudes to about 8 km near the poles. These statements are a practical definition of the tropopause appropriate for today's climate on Earth — they would not hold on another planet or in a changed climate. Regardless, the tropopause is a distinct boundary separating two differently stratified regions, the troposphere and the stratosphere. The thermal tropopause is marked in Fig. 15.22 and, as we see there and in Fig. 15.16, in the extratropics it is almost parallel to isolines of potential vorticity, and sometimes an isoline of potential vorticity (say  $Q = 3$  or 4 PV units) is used as a somewhat ad hoc definition of the extratropical tropopause.

Finally we note that the tropopause appears as a rather sharp feature when viewed instantaneously, although this sharpness is often blurred when time or spatial averages are taken. The solid line in Fig. 15.24, denoted 'tropopause-based average', shows the profile obtained when the tropopause height itself is taken as a common reference level, using data from individual radiosonde ascents over the United States.<sup>9</sup> The sharpness may indicate that the tropopause is acting as a mixing barrier for potential vorticity, separating the better-mixed troposphere and the more quiescent stratosphere.



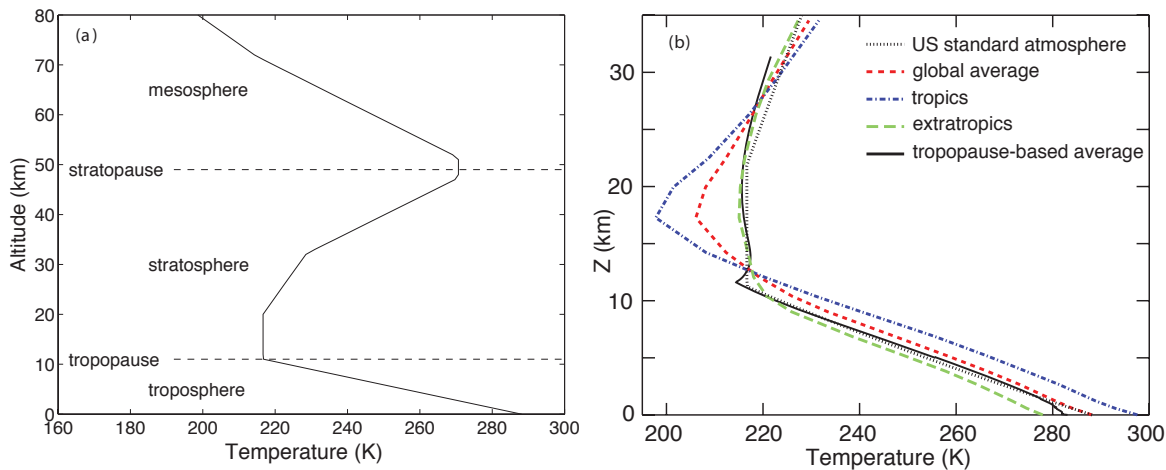


**Fig. 15.24** (a) The temperature profile of the 'US standard atmosphere', marking the standard regions of the atmosphere below 80 km. In addition to the regions shown, the top of the mesosphere is marked by the mesopause, at about 80 km, above which lies the 'thermosphere', in which temperatures rise again into the 'exosphere', extending a few thousand kilometres and where the atmospheric temperature ceases to have a useful meaning. (b) Observed, annually averaged profiles of temperature in the atmosphere, where the ordinate is log-pressure. 'Tropics' is the average from 30° S to 30° N, and the extratropics is the average over the rest of the globe. The observations are from a reanalysis over 1958–2003 that extends upwards to about 35 km. See text for the meaning of 'tropopause-based average'.

### 15.5.1 Baroclinic Eddies and the Maintenance of Stratification

The atmosphere is largely heated at the surface – the ground is heated by the Sun and the ground heats the atmosphere. If the air near the surface becomes too warm it will become convectively unstable and the resulting convection (here meaning predominantly vertical convection occurring on relatively small scales) will transport heat upwards, stabilizing the temperature profile. If we look at the temperature profiles in Fig. 15.25 we see that in the tropics and subtropics the lapse rate is very close to the saturated adiabatic lapse rate, which is the lapse rate that is neutrally stable to convection in the presence of moisture (as we consider further in Chapter 18), suggesting that the stratification is indeed maintained by convection. But in mid- and high latitudes the lapse rate is quite stable with respect to convection, suggesting that some process other than convection is transporting heat upwards. The obvious candidate is baroclinic instability because that has the property of transporting heat both poleward and upward, both of which occur in the atmosphere, and if the vertical transport is efficient enough convection will then not be needed.

The baroclinic eddies do not extend infinitely upwards, and so we expect a boundary — a *tropopause* — between a dynamical troposphere and a stratosphere that is more nearly in radiative equilibrium. That is to say, the troposphere is that region in which a dynamical distribution of energy takes place; in the tropic this redistribution is by convection, and in mid-latitudes the redistribution is effected by baroclinic eddies. Given this picture, two questions present themselves:

- (i) What determines the stratification (i.e., the lapse rate) of the mid-latitude troposphere?
- (ii) What determines the height of the tropopause?

The full answer to these questions involves both radiation and dynamics. In the following sections, we will focus more on dynamics, and in Section 15.6 we will bring radiation into the mix. However, we won't discuss radiation itself until Chapter 18, so the reader who desires a full understanding will have to skip back and forth a little.



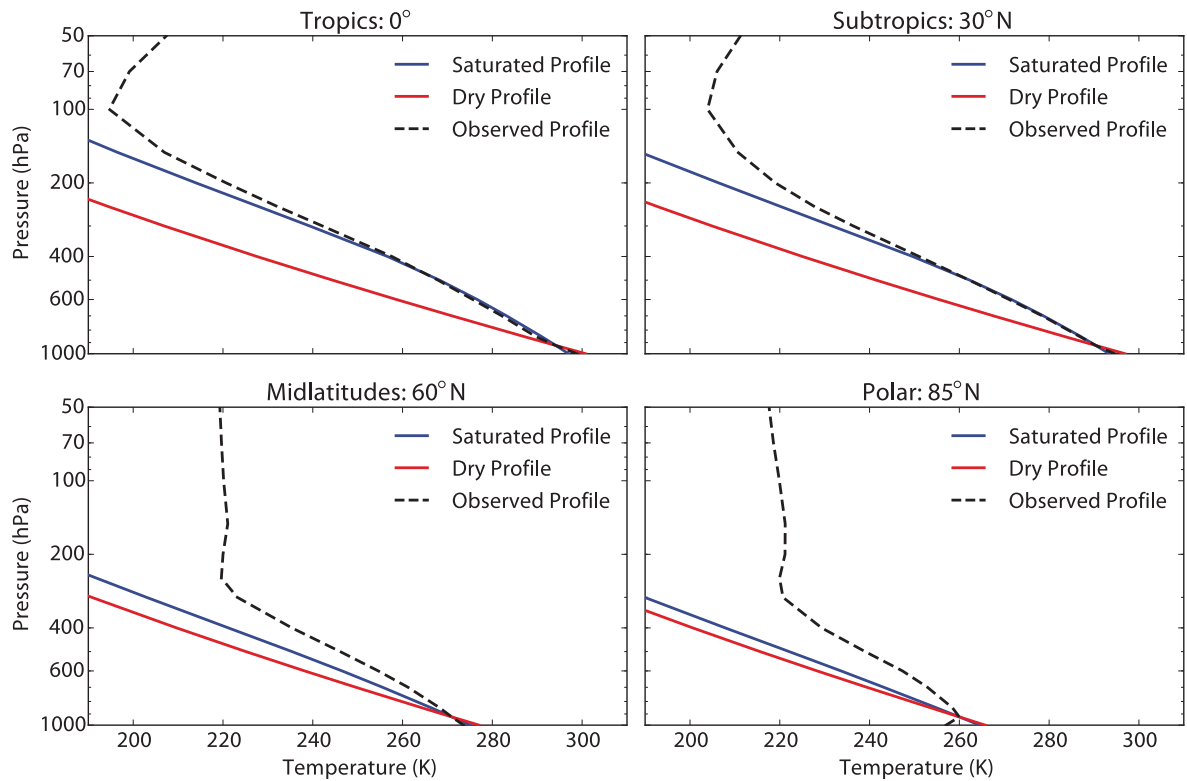


**Fig. 15.25** The annually- and zonally-averaged observed (from reanalysis) temperature profiles at various latitudes, along with profiles constructed by integrating the saturated and dry adiabatic lapse rates, chosen to coincide with the observed temperature at 925 hPa, or about 750 m.

### 15.5.2 † Potential Vorticity Mixing and Baroclinic Adjustment

Baroclinic eddies grow from small beginnings to finite amplitude, and it is the finite amplitude eddies that stir the atmosphere and define the troposphere. However, they do not forget their linear properties, so let us remind ourselves of one.

#### *A linear height scale*

On the  $\beta$ -plane, linear baroclinic instability can produce a height scale that is different from the height of any pre-existing 'lid' or from the density scale height. This height scale is (Section 9.9.1)

$$h = \frac{\Lambda f^2}{\beta N^2}, \quad (15.110)$$

where  $\Lambda = \partial \bar{u} / \partial z$ . That is to say, if  $h < H$ , where  $H$  is the density scale height (or the height of some lid in a Boussinesq model), then the baroclinic eddies will extend upwards to a height  $h$ , and this will be the vertical extent of significant heat fluxes. Thus (one might argue), below  $h$  the thermal structure is determined by the dynamical effects of baroclinic instability, whereas above  $h$  the atmosphere is more nearly in radiative equilibrium. Using  $\Lambda = (15 \text{ m s}^{-1}) / (10 \text{ km})$ ,  $\beta = 1.6 \times 10^{-11} \text{ s}^{-1} \text{ m}^{-1}$ ,  $f = 1 \times 10^{-4} \text{ s}^{-1}$  and  $N = 10^{-2} \text{ s}^{-1}$  gives  $h \approx 10 \text{ km}$ , which approximates the height of the tropopause in mid-latitudes. This is not a prediction because we have taken observed values for the stratification and shear. The amplitude of meridional heat transfer, which determines the meridional temperature gradient and so the shear  $\Lambda$ , is really determined by nonlinear effects.

### Mixing

Let us now suppose that baroclinic eddies grow to finite amplitude and mix potential vorticity (see Section 13.5 for a general discussion of potential vorticity mixing). Such mixing will try to homogenize potential vorticity, or equivalently to expel potential vorticity gradients to a boundary, and if so the (extratropical) tropopause will occur at an isoline of potential vorticity, and be marked by a near-discontinuity in the potential vorticity distribution. Because  $Q \approx (f/\rho)\partial\theta/\partial z$ , the tropopause would also correspond to a discontinuity in stratification. These ideas are, at least qualitatively, in accord with observations: the potential vorticity distribution in the troposphere is somewhat more homogeneous than in the stratosphere — see Fig. 15.16, noting the unequal contour intervals of PV, and there is a near-discontinuity in stratification (by definition) at the tropopause. What are the effects of that mixing?

Potential vorticity mixing will occur only so far as needed in order to stabilize the mean flow. We also know that the meridional surface temperature gradient remains negative, so that if the flow is stabilized it must involve changes in the interior potential vorticity distribution. If horizontal scales are sufficiently large we may neglect the contribution of relative vorticity, and the quasi-geostrophic potential vorticity and its gradient become

$$q = \beta y + \frac{\partial}{\partial z} \left( \frac{f_0^2}{N^2} \frac{\partial \psi}{\partial z} \right) \quad \text{and} \quad \frac{\partial \bar{q}}{\partial y} = \beta - \frac{\partial}{\partial z} \left( \frac{f_0^2}{N^2} \Lambda \right). \quad (15.111)$$

We might hypothesize that the vertical extent to which mixing occurs is just sufficient to make the two terms on the right-hand side a similar size in order that the potential vorticity can become homogeneous, or that it can change sign and be just unstable. This gives  $\beta \sim f_0^2 \Lambda / (N^2 H_T)$ , where  $H_T$  is the vertical extent of the instability and, we assume, the height of the tropopause; that is

$$H_T \sim \frac{f_0^2 \Lambda}{N^2 \beta}. \quad (15.112)$$

Put another way, in this model *the troposphere extends vertically as far as baroclinic waves can alter the potential vorticity from its planetary value*. (A similar depth scale occurs when evaluating the depth of the wind's influence in an ocean circulation model, Section 20.2.1.) If the lapse rate (and the shear) is known, this height determines the tropopause. Note the similarity of (15.112) to (15.110) — a similarity that is unsurprising given that we are constructing a height scale from a shear,  $f$ ,  $\beta$  and  $N^2$  using potential vorticity dynamics in both cases. We still do not have a prediction for  $H_T$ , because the stratification  $N^2$  is unknown.

### Baroclinic adjustment

Equilibration by potential vorticity mixing is closely related to a process known as *baroclinic adjustment*, by analogy with convective adjustment. The essential idea is that baroclinic eddies are sufficiently efficient that they can stabilize the mean flow by transferring heat poleward and upward until the necessary condition for instability (the Charney–Stern–Pedlosky condition, in so far as the flow is quasi-geostrophic and inviscid) is just satisfied, and the atmosphere is marginally supercritical to baroclinic instability. The adjustment might conceivably proceed predominantly by changes in the static stability,  $N^2$ , or predominantly by changes in the horizontal temperature gradient. The arguments for such an adjustment process are a little ad hoc, and the final state to which the atmosphere putatively adjusts is not well-defined since there is no critical shear for instability in a continuously stratified model. In a two-level model the critical shear for instability is given by (9.121), which may be put in the form

$$\Lambda_{\text{crit}} = \frac{\beta N^2 H}{f_0^2}, \quad (15.113)$$

which is of the same form as (15.112). In a continuously stratified model, (15.113) may be regarded as a value of the shear above which the baroclinic eddies become deep (all eddies are deep in the two-level model) and transport heat efficiently.

Allowing the parameters  $f$  and  $\beta$  to vary with latitude, and using the thermal wind relation, (15.112) or (15.113) may be written in the form

$$H_T = - \left( \frac{\partial_y \theta}{\partial_z \theta} \right) \frac{f}{\beta} = s \frac{f}{\beta} \sim sa, \quad (15.114)$$

where  $s = -(\partial_y \theta)/(\partial_z \theta)$  is the isentropic slope and  $a$  is the Earth's radius. This equation suggests that the isentropic slope is roughly such that isentropes extend from the surface in the subtropics to the tropopause at the poles, and this is more-or-less true in the present atmosphere (Fig. 15.16). That is to say, if adjustment-like arguments do hold, the isentropic slope will remain roughly constant even as other parameters change — for example, the horizontal temperature gradient may change with season but the stratification changes such as to keep  $s$  the same. The numerical and observational evidence for such an adjustment is mixed, although it is plausible that a weaker version may hold in which potential vorticity is imperfectly homogenized and (15.112) provides a plausible scaling, but not a precise prediction.<sup>10</sup>

Even if the above scalings were correct, they provide a closed prediction of neither the tropopause height nor stratification; they only provide a relation between the two. We will close the problem in Section 15.6, but first we consider another point of view.

### 15.5.3 † Extratropical Convection and the Ventilated Troposphere

A point of view that differs *qualitatively* from the potential vorticity one is to suppose that the mid-latitude tropospheric lapse rate is maintained by convection, the convection occurring predominantly in the warm sector of mature baroclinic waves.<sup>11</sup> In reality such convection will involve moisture, but first consider a dry atmosphere. In a given baroclinic zone the minimum potential temperature difference between the tropopause and the surface,  $\Delta_z \theta = \theta_T - \theta_S$  is approximately zero: if the tropopause were colder than this the column would be convectively unstable, and the difference would become zero. The essential assumption that we make is that within a baroclinic zone there generally *does* exist a region that is convectively unstable, and that convection then ensues with sufficient efficiency to partially fill the troposphere with air with that surface value of potential temperature. The process differs from convection in the tropics because it is organized by baroclinic waves and, if we imagine a succession of baroclinic waves around a latitude band the mean value of  $\Delta_z \theta$  will be approximately, we assume, its minimum (zero) plus a fraction of its standard deviation. The standard deviation in turn is a consequence of the pre-existing meridional temperature gradient and meridional advection across that gradient, and therefore

$$\text{standard deviation}(\Delta_z \theta) \propto \Delta_y \theta, \quad (15.115)$$

where the term on the right-hand side is the meridional temperature difference at the surface across the baroclinic zone. The mean potential temperature difference between the surface and tropopause is then simply proportional to the meridional temperature gradient at that latitude, with an undetermined constant of proportionality and so

$$\Delta_z \theta \propto \Delta_y \theta. \quad (15.116)$$

Finally, if moisture is present (as it is!) the potential temperature should be replaced by the equivalent potential temperature — the potential temperature achieved when all the water vapour in a parcel of air condenses and the latent heat of condensation is used to heat the parcel (Section 18.3.2).

The physical hypothesis is essentially that within a baroclinic wave the advection of warm air into a cold region *necessarily* leads to convection, and that this convection then efficiently fills the

### The Stratification of the Troposphere and Stratosphere

- The troposphere is that region of the atmosphere in which a dynamical redistribution of heat occurs. The stratosphere above it is more nearly in radiative equilibrium (although in winter in the lower stratosphere, radiative equilibrium is not a very good approximation). The tropopause is the change in stratification between the two regions.
- The tropospheric lapse rate and the height of the tropopause are determined by a combination of dynamics and radiation. The tropopause temperature is, to a fair approximation, determined by the requirements of radiative balance and the height of the tropopause then follows if the lapse rate is known, and vice versa. Dynamical and radiative consistency leads to a state in which the tropopause height is the height to which dynamical effects extend and equal to the height needed for radiative balance.
- In Earth's atmosphere, there are two dynamical processes important for the maintenance of stratification:
  - (i) *Convection, especially moist convection.* It is generally thought that moist convection plays the dominant role in determining tropical stratification, leading to a lapse rate that is approximately neutral to moist convection (discussed more in Chapter 18).
  - (ii) *Baroclinic eddies.* In mid-latitudes baroclinic eddies transport heat poleward and upwards, so determining in the mid-latitude meridional temperature gradient and stratification. Various theories for this have been proposed, but none are accepted as having wide applicability and accuracy. In one incarnation ('baroclinic adjustment') baroclinic activity is so efficient that the atmosphere becomes only marginally supercritical to baroclinic instability, a process related to homogenization of potential vorticity. In a variation on this theme, potential vorticity and surface potential temperature are diffused downgradient, but potential vorticity is not necessarily homogenized. A complete theory would require estimates of the structure and magnitude of the eddy diffusivities.

In the extratropics moist convection is less dominant, but convection in the warm sector of baroclinic eddies may act to produce a stratification that is related to the meridional temperature difference across a baroclinic zone.

- If we have a theory for the stratification produced by baroclinic eddies then we can use that theory in conjunction with radiative calculations to make predictions of the tropopause height, as in Section 15.6. For example, various dynamical arguments suggest the importance of the height scale  $H \sim (f^2 \Lambda)/(N^2 \beta)$ , where we associate  $H$  with the tropopause height. Radiative arguments also lead to an expression for tropopause height in terms of the stratification. Using the two together gives predictions for both tropopause height and the stratification.
- In the mid-stratosphere, ozone absorbs solar radiation and this gives rise to an increase in temperature with height from the lower- to the mid-stratosphere. This effect makes the stratosphere still more stable to baroclinic instability and may sharpen the tropopause, but it is not the root cause of the tropopause.

available volume, to the extent possible, with the warmest possible fluid. Oceanographers will find this a comfortable concept, for they are used to the notion of convection filling the domain with the densest available fluid (densest in the oceanic case because oceanic convection usually occurs from the top, with cold, dense water sinking). However, unlike the ocean in which the bottom of the container limits the volume of dense water that can be made, here it is the tropopause that provides the upper lid; the height of this is determined by the dynamics itself, in conjunction with the requirement of radiative balance. Thus, the baroclinic zone becomes, in oceanographic parlance, *ventilated* by the warmest air at the surface. However, the entire baroclinic zone does not completely fill with this warm air because the convection is maintained by a meridional temperature gradient and it is necessarily intermittent: baroclinic instability would shut off if the entire baroclinic zone were filled with homogeneous warm fluid, and the zone would then meridionally restratify. It is this continual maintenance of variance that leads to (15.116).

The ultimate consequence of these convection arguments is that the moist isentropic slope is proportional to that slope which would take an isentrope at the surface to the tropopause across a baroclinic zone. On Earth, this is similar to the potential vorticity mixing ideas, which suggest that the isentropic slope is proportional to the slope that goes from the ground to the tropopause over a horizontal scale  $f/\beta$ , the equator-to-pole scale, but the reasons are different.

### 15.6† A MODEL FOR BOTH STRATIFICATION AND TROPOPAUSE HEIGHT

In the previous section we discussed various ideas regarding the effects of baroclinic eddies on the mid-latitude stratification. The discussion was incomplete on two grounds. First, the ideas themselves are heuristic. Second, even if true, they don't give us a complete picture; they just give us a relation between stratification and tropopause height. A second relation is needed, and this is provided by the radiative-dynamical arguments of Section 18.6 and Appendix C of Chapter 18, which the reader may now read with profit. In those sections we showed that, if the lapse rate in the lower atmosphere is assumed constant, it can extend upward only to a certain height in order to maintain an overall radiative balance — that is, in order that the outgoing longwave radiation equal the incoming solar radiation. Specifically, we obtained an approximate analytic expression for the tropopause height,  $H_T$ , (18.172), namely

$$8\Gamma H_T^2 - C H_T T_T - \tau_s H_a T_T = 0. \quad (15.117)$$

where  $C = 2 \log 2 \approx 1.39$ . In this expression  $\Gamma$  is the lapse rate,  $-\partial T/\partial z$ ,  $T_T$  is the temperature at the tropopause,  $\tau_s$  is the surface optical depth and  $H_a$  is the scale height of the main infrared absorber. The radiative parameters are determined by the composition of the atmosphere and we regard them as given, and the temperature at the tropopause is, to a decent approximation, given by radiative balance, namely  $2\sigma T_T^4 \approx S_{net}$  where  $S_{net}$  is the net incoming solar radiation. (If there is a lateral convergence of heat in the atmosphere then  $S_{net}$  should be modified appropriately. Alternatively, we regard (15.117) as a theory for the global mean tropopause height.) The main assumptions leading to (15.117) are that the atmosphere is radiatively grey in the infrared and that the lapse rate is uniform up to  $H_T$ .

In mid-latitudes, (15.117) does not provide a closed prediction for tropopause height because the lapse rate is not known (whereas in the tropics we might take the lapse rate to be determined by convection). However, if we combine (15.117) with the ideas about baroclinic transport we obtain a closed model. We do not have a good model of baroclinic transport, but for the purposes here let us suppose that the isentropic slope is such that (15.114) roughly holds. Noting that, in a hydrostatic atmosphere,  $(T/\theta) \partial \theta / \partial z = \Gamma_d - \Gamma$  where  $\Gamma_d$  is the dry adiabatic lapse rate, we rewrite (15.114) as

$$\Gamma = \Gamma_d + \left( \frac{\partial_y T}{H_T} \right) \frac{f}{\beta}. \quad (15.118)$$

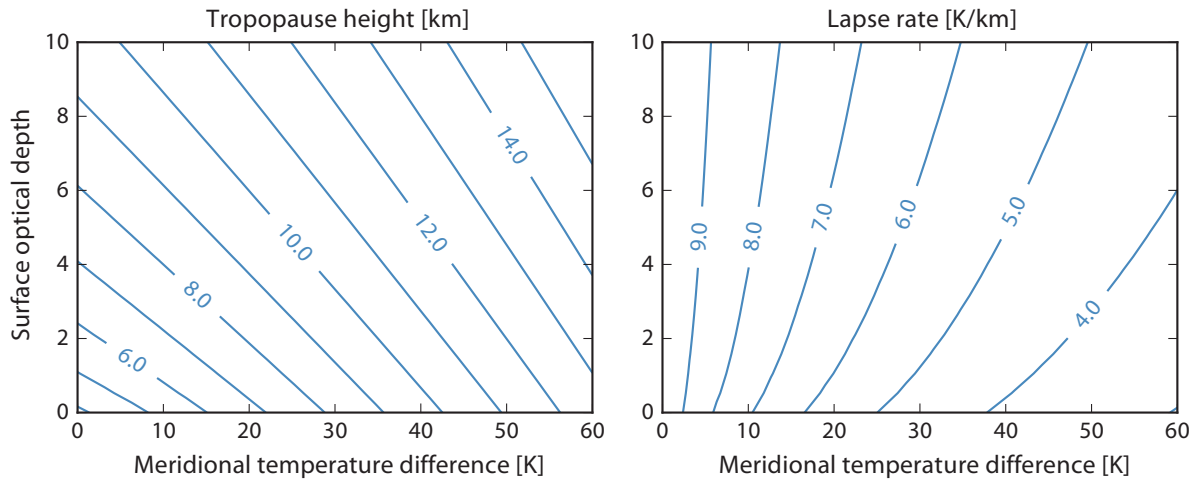


**Fig. 15.26** Left: Contours of tropopause height as a function of the temperature difference between the subtropics and pole, and the optical depth. Right: Corresponding lapse rate,  $-\partial T/\partial y$ . The results are from a theoretical calculation using (15.120) and (15.118), here with  $H_a = 2$  km and a tropopause temperature of 215 K.

If we take  $H_T \approx 10$  km and  $\partial T/\partial y \approx 40$  K/(7000 km) we obtain not-unreasonable values for  $\Gamma$  of around  $4 \text{ K km}^{-1}$ .

If we suppose that both (15.117) and (15.118) are true we obtain predictions for the height of the tropopause in mid-latitudes and the tropospheric stratification, as a function of the horizontal temperature gradient and the radiative properties of the atmosphere. In doing so we are saying the following, in rather general terms. *The height of the tropopause is the height to which baroclinic eddies extend, and it is also the height demanded by radiative balance.* The simultaneous satisfaction of these two conditions provides predictions for both the tropopause height and the lapse rate. The theory is not complete, because the lateral temperature gradient is not predicted, and this is a function of the efficiency of baroclinic eddies. It is also the case that we have chosen a particular closure for baroclinic eddies that may not have general applicability. If we had a better theory we would use it instead, and the reader is invited to explore other options.

### 15.6.1 Some Calculations

If we combine (15.118) and (15.117) we obtain

$$8\Gamma_d H_T^2 - H_T \left[ C T_T - \left( \frac{8f\partial_y T}{\beta} \right) \right] - \tau_s H_a T_T = 0, \quad (15.119)$$

the solution of which is

$$H_T = \frac{1}{16\Gamma_d} \left( A + \sqrt{A^2 + 32\Gamma_d \tau_s H_a T_T} \right), \quad (15.120)$$

where  $A = C T_T - 8f\partial_y T/\beta$ . The solutions are plotted in Fig. 15.26, but it may help interpret these if we consider the optically thin and thick cases, namely

$$\text{Optically thick: } \tau_s H_a \gg \frac{A^2}{32\Gamma_d T_T} \quad \text{whence} \quad H_T \approx \sqrt{\frac{T_T \tau_s H_a}{8\Gamma_d}}, \quad (15.121)$$

$$\text{Optically thin: } \tau_s H_a \ll \frac{A^2}{32\Gamma_d T_T} \quad \text{whence} \quad H_T \approx \frac{C T_T - 8\partial_y T f/\beta}{8\Gamma_d}. \quad (15.122)$$



The optically thin case shows the effects of baroclinic eddies. If the horizontal heat transport is very strong and  $\partial T/\partial y$  is small then the lapse rate will approach the dry adiabat and the tropopause height will diminish, and conversely for a weak heat transport. Solutions to the full problem show that behaviour, as well as a slight increase in height with optical depth, because with bigger optical depth the effective emitting level is higher, and the tropopause height tracks the emitting level.

The solutions are qualitatively reasonable, but we repeat some caveats. On the radiative side the atmosphere is not grey, although that is a quantitative rather than qualitative deficiency. On the dynamical side we have used an ansatz — that the isentropic slopes are fixed — that we believe not to be exactly true and even this is not a complete treatment of baroclinic activity, since it does not give us the horizontal temperature gradient. Notwithstanding these points, the calculation does capture a fundamental principle, that the tropopause height and stratification are determined by the joint effects of dynamics and radiation. Finally, the stratosphere is quite stably stratified and this strongly inhibits baroclinic instability. Thus, once formed by the mechanisms above, the tropopause provides a natural lid on baroclinic instability, keeping it tropospherically confined.

## APPENDIX A: TEM FOR THE PRIMITIVE EQUATIONS IN SPHERICAL COORDINATES

In spherical and log-pressure coordinates let us define the residual streamfunction for the ideal-gas primitive equations by<sup>12</sup>

$$\psi^* \equiv \psi + \frac{\overline{v'\theta'}}{\partial_Z \bar{\theta}}. \quad (15.123)$$

Here, an overbar denotes a conventional (Eulerian) zonal average,  $\psi$  is the streamfunction of the zonally-averaged flow,  $Z = -H \ln(p/p_R)$  where  $p_R$  is a reference pressure and  $H$  is a scale height, and  $\rho_R = \rho_0 \exp(-Z/H)$  where  $\rho_0$  is a constant. The associated transformed, or residual, velocities are:

$$\bar{v}^* = -\frac{1}{\rho_R} \frac{\partial}{\partial Z} (\psi^* \rho_R), \quad \bar{w}^* = \frac{1}{a \cos \vartheta} \frac{\partial}{\partial \vartheta} (\psi^* \cos \vartheta), \quad (15.124)$$

with an equivalent expression for  $\bar{v}$  and  $\bar{w}$  in terms of  $\psi$ . (The notation for log-pressure coordinates follows Section 2.6.3 on page 82, except here we use a lowercase  $w$  for the vertical velocity.) If we write the equations of motion in terms of the residual velocities instead of the Eulerian velocities we obtain the ‘transformed Eulerian mean’, or TEM, equations (section 10.3). The TEM forms of the zonally-averaged thermodynamic and zonal momentum equations are:

$$\frac{\partial \bar{\theta}}{\partial t} + \frac{\bar{v}^*}{a} \frac{\partial \bar{\theta}}{\partial \vartheta} + \bar{w}^* \frac{\partial \bar{\theta}}{\partial Z} = \frac{1}{\rho_R} \frac{\partial G}{\partial z}, \quad (15.125a)$$

$$\frac{\partial \bar{u}}{\partial t} + \bar{v}^* \left( \frac{1}{a \cos \vartheta} \frac{\partial}{\partial \vartheta} (\bar{u} \cos \vartheta) - f \right) + \bar{w}^* \frac{\partial \bar{u}}{\partial Z} = \frac{1}{\rho_R \cos \vartheta} \nabla \cdot \mathcal{F}. \quad (15.125b)$$

The transformed equations of motion are completed by the meridional momentum, mass continuity and hydrostatic equations:

$$\bar{u} \left( f + \frac{\bar{u}}{a} \tan \vartheta \right) = -\frac{1}{a} \frac{\partial \Phi}{\partial \vartheta} + \hat{S}, \quad (15.126a)$$

$$\frac{1}{a \cos \vartheta} \frac{\partial}{\partial \vartheta} (\bar{v}^* \cos \vartheta) + \frac{1}{\rho_R} \frac{\partial}{\partial Z} (\rho_R \bar{w}^*) = 0, \quad (15.126b)$$

$$\frac{\partial \Phi}{\partial Z} = \frac{R \bar{T}}{H} T = \frac{R}{H \bar{\theta}} e^{-\kappa Z/H}. \quad (15.126c)$$



In (15.125b),  $\mathcal{F} = (\mathcal{F}^\vartheta, \mathcal{F}^Z)$  is the Eliassen–Palm flux, given by

$$\mathcal{F}^\vartheta = \rho_R \cos \vartheta \left[ \bar{u}_Z \frac{\overline{v'\theta'}}{\partial_Z \bar{\theta}} - \overline{u'v'} \right], \quad (15.127a)$$

$$\mathcal{F}^Z = \rho_R \cos \vartheta \left[ \left( f - \frac{\partial_\vartheta(\bar{u} \cos \vartheta)}{a \cos \vartheta} \right) \frac{\overline{v'\theta'}}{\partial_Z \bar{\theta}} - \overline{u'w'} \right], \quad (15.127b)$$

with

$$\nabla \cdot \mathcal{F} = \frac{1}{a \cos \vartheta} \frac{\partial}{\partial \vartheta} (\mathcal{F}^\vartheta \cos \vartheta) + \frac{\partial}{\partial Z} \mathcal{F}^Z. \quad (15.127c)$$

In (15.125a)

$$G = \frac{\rho_R}{\partial_Z \bar{\theta}} \left( \overline{v'\theta'} \frac{1}{a} \frac{\partial \bar{\theta}}{\partial \vartheta} + \overline{w'\theta'} \frac{\partial \bar{\theta}}{\partial Z} \right), \quad (15.127d)$$

and  $\hat{S}$  in (15.126a) contains various, generally small, terms that lead to departures from gradient-wind balance between  $\bar{u}$  and the geopotential  $\Phi$ . Expressions very similar to the ones above also arise in pressure coordinates.

In many circumstances, the EP flux is well approximated by

$$\mathcal{F} = \left( -\rho_R \cos \vartheta \overline{u'v'}, f \rho_R \cos \vartheta \frac{\overline{v'\theta'}}{\partial_Z \bar{\theta}} \right), \quad (15.128)$$

in which case the zonal flow is accelerated by the EP flux according to

$$\frac{\partial \bar{u}}{\partial t} + \dots = \frac{1}{a \cos^2 \vartheta} \frac{\partial}{\partial \vartheta} \left( -\overline{u'v'} \cos^2 \vartheta \right) + \frac{1}{\rho_R} \frac{\partial}{\partial Z} \left( \rho_R f \frac{\overline{v'\theta'}}{\partial_Z \bar{\theta}} \right). \quad (15.129)$$

With  $f = f_0$  (15.128) becomes the quasi-geostrophic EP flux, and in this limit  $G$  is also neglected.

In the figures that show the EP vectors, the horizontal and vertical components of the EP flux are scaled by  $a$  (the Earth's radius) and by  $H = 1000$  hPa (the pressure depth of the atmosphere), respectively. The scaling determines the direction of the arrows and makes it possible to see the divergence by eye, and which component dominates in producing that divergence. In the figures that show the EP flux divergence, we plot the right-hand side of (15.125b), namely the EP flux divergence divided by  $\rho_R \cos \vartheta$ , this being the quantity that directly contributes to the acceleration of the zonal flow.<sup>13</sup>

## Notes

- 1 The modern view of the mid-latitude general circulation — of a largely zonally-asymmetric motion that provides the bulk of the meridional transport of heat and momentum in the extratropics — began to take form in the 1920s in papers by Defant (1921) and Jeffreys (1926). Defant regarded the mid-latitude circulation as turbulence on a large scale (albeit without realizing the important organizing effects of waves), and calculated the horizontal eddy-diffusivities using Prandtl-like mixing length arguments. Soon after, Jeffreys presciently wrote of 'the dynamical necessity for a continual exchange of air between high and low latitude' and that 'no general circulation of the atmosphere without cyclones is dynamically possible when friction is taken into account.' This point of view slowly gained ground, with, for example, Starr (1948) advocating the point of view that large-scale eddies were responsible for the bulk of the meridional transport of momentum in mid-latitudes, and Rossby (1949) eventually noting in a review article that 'One is forced to conclude that there no

longer exists a compelling reason to build the theory of the maintenance of the general circulation exclusively on *meridional* solenoidal circulations'.

Following this work came a pair of discussion papers by Eady (1950, 1954), that, setting the stage for the modern viewpoint, struggle with the turbulent transport of mid-latitude eddies and the maintenance of the surface currents — the importance of the enstrophy budget is discussed, for example, and Eady comes close to deriving wave activity conservation. Around that time Kuo (1951) discussed the maintenance of zonal flows by the mechanism of vorticity transfer in a state with a meridional background gradient, similar to mechanism I of Section 15.1.2. Another milestone was the influential monograph by Lorenz (1967) that synthesized the progress to that date, noting (in his last paragraph) that the cause of the poleward eddy momentum transport across mid-latitudes (and hence the cause of the surface eastward winds) had not at that time been rigorously explained. If perhaps not rigorous, we do now have a qualitative explanation of these dynamics by way of potential vorticity dynamics and the momentum transport in Rossby waves, as described in this chapter and in Chapter 10.

- 2 The mechanism producing a westerly jet in the atmosphere, and the associated surface westerlies, used to be referred to as 'negative viscosity' (Starr 1968), because it is associated with an upgradient transfer of momentum. The generation of a zonal flow by rearrangements of vorticity on a background state with a meridional gradient was noted by Kuo (1951). Dickinson (1969) and Thompson (1971, 1980) calculated the momentum transport by Rossby waves, with Thompson explicitly noting that the zonal momentum flux was in the opposite direction to the group velocity. There is thus a potential for upgradient transfer and mean flow generation, as experimentally verified by Whitehead (1975). These ideas were developed further by Green (1970), Rhines & Holland (1979) and others since.
- 3 This technique is noted by Lighthill (1965), who remarks that the idea goes back to Rayleigh.
- 4 Following Held (2000).
- 5 Models of the general circulation of this ilk were introduced by Green (1970). Dickinson (1969) also considered the potential vorticity transport in planetary waves.
- 6 Adapted from Jukes (2001).
- 7 Early evidence that the temperature increases above about 11 km came from the balloon measurements of Tesserenc De Bort (1902), who also suggested the names tropopause and stratosphere, and Assmann (1902). See Hoinka (1997) for a historical account. More recently, radiative and dynamical issues relevant to this topic are discussed by, among others, Stone (1972), Held (1982), Jukes (2000) and some of the articles in Schneider & Sobel (2007), and we draw on many of them.
- 8 Paraphrasing World Meteorological Organization (1957); see also Lewis (1991).
- 9 Thomas Birner calculated the tropopause-based averages. See also Birner *et al.* (2002) and Birner (2006).
- 10 In some but not all circumstances it seems that rotating fluids do seek to become marginally supercritical, in some sense, to baroclinic instability. The original suggestion ('baroclinic adjustment') was due to Stone (1978), and Stone & Nemet (1996) found that the isentropic slope of the real atmosphere does not vary strongly with season, even though the heat flux does, a result supportive of baroclinic adjustment ideas. Related to this (although their interpretation and reasoning were different) Schneider & Walker (2006) found that an idealized model atmosphere was only marginally supercritical over a broad parameter regime. However, other simulations have found examples of supercritical flows. Salmon (1980) and Vallis (1988b) found that quasi-geostrophic flow could be strongly supercritical, and Thuburn & Craig (1997) and Zurita-Gotor & Vallis (2009, 2011) found results that were not supportive of baroclinic adjustment in primitive equation models. In Earth's atmosphere linear calculations show that the mean atmospheric state, certainly in winter, is baroclinically unstable, with growth rates of about  $0.2 \text{ day}^{-1}$  or more (Valdes & Hoskins 1988), and the Eady growth rate is similarly positive over a large fraction of the mid-latitudes. See Zurita-Gotor & Lindzen (2007) for a review of some of these ideas. Jansen & Ferrari (2012, 2013) discussed and modelled the reasons for the various differences, and concluded that marginal criticality is not a

general property of a rotating stratified system. It is likely that much of Earth's ocean is supercritical. Nevertheless, the idea is one we use in Section 15.6.

- 11 Following Jukes (2000).
- 12 For more detail see Edmon *et al.* (1980) or Andrews (1987).
- 13 E. Gerber kindly constructed these figures.